Review of Materials Research 1 (2025) 100019

Contents lists available at ScienceDirect

Review of Materials Research

journal homepage: www.sciencedirect.com/journal/review-of-materials-research

Breaking the strength-ductility trade-off for metal matrix composites: A review of the role of nanoscale reinforcement dimension on the deformation and strengthening mechanisms

Yuhang Xia [a,b], Xiang Zhang [a,b,*], Dongdong Zhao [a,b], Xudong Rong [a,b], Chunnian He [a,b,c,d], Naiqin Zhao [a,b,c,d]

[a] School of Materials Science and Engineering, Tianjin Key Laboratory of Composite and Functional Materials, Tianjin University, Tianjin, 300072, China
[b] State Key Laboratory of Precious Metal Functional Materials, Tianjin University, Tianjin, 300072, China
[c] Key Laboratory of Advanced Ceramics and Machining Technology (Ministry of Education), Tianjin University, Tianjin, 300072, China
[d] Collaborative Innovation Center of Chemical Science and Engineering (Tianjin), Tianjin, 300072, China

ARTICLE INFO

Keywords:
Metal matrix composites
Strength-ductility trade-off
Strengthening and toughening mechanisms
Reinforcement dimension
Deformation behavior

ABSTRACT

Metal matrix composites (MMCs) reinforced by various dimensional nanoscale reinforcements (ranging from 0D to 3D) have gained significant importance in numerous fields such as electronic circuits, aerospace and new energy vehicles due to their exceptional mechanical and functional properties. Despite their widespread applications, the inherent disparity in properties between the matrix and nanoscale reinforcements often results in a trade-off between strength and plasticity, as well as diminished physical characteristics. This dilemma significantly impedes the advancement of MMCs. This review aims to discuss the current state of research on MMCs reinforced by nanoscale reinforcements, highlighting the intricately designed approaches for achieving high strength-ductility matching or enhanced physical properties. Furthermore, the review systematically examines the factors influencing strengthening, toughening mechanisms and deformation behavior, as supported by current experimental and theoretical research across various reinforcement dimensions. Analyzing and evaluating the internal mechanisms and influencing factors that govern the distinctive dimensional design to achieve specific properties can provide fundamental principles for designing and fabricating high-performance composite materials, facilitating the extensive application of the MMCs in cutting-edge fields such as aerospace, electronic communications, and artificial intelligence.

1. Introduction

The rapid advancement in technology and industrial processes has brought new opportunities and challenges to the field of materials science, particularly in metallic materials, regarding their excellent mechanical, thermal, electrical, electrochemical, and biomedical properties. Benefiting from the great flexibility for the selection of the reinforcements and microstructure design, metal matrix composites (MMCs) are identified as an optimal choice for surpassing the inherent performance limitations in traditional metals and their alloys. In recent years, MMCs reinforced with zero-dimensional (0D) nanoparticles, one-dimensional (1D) nanotubes/nanofibers, two-dimensional (2D) nanoplates/nanosheets and three-dimensional (3D) continuous network have exhibited tremendous improvement in the strength and hardness [1–3]. However, the incorporation of nanoscale reinforcements into MMCs often leads to unpredictable effects on other properties, such as ductility and electrical/thermal conductivity. For instance, the significant disparity in the inherent properties of both reinforcements and matrix makes achieving proper dispersion of nanoscale reinforcements very challenging, potentially causing agglomeration issues that degrade ductility or fracture toughness. Additionally, inadequate interfacial wettability can result in weak interaction or poor load transfer between reinforcements and matrix, further complicating the enhancement of overall performance enhancement [4,5]. These issues collectively contribute to a strength-ductility trade-off and the degradation of the physical properties of the composites. Furthermore, the heterogeneous

* Corresponding author. School of Materials Science and Engineering, Tianjin Key Laboratory of Composite and Functional Materials, Tianjin University, Tianjin, 300072, China.
E-mail address: zhangxiang@tju.edu.cn (X. Zhang).

https://doi.org/10.1016/j.revmat.2025.100019
Received 21 March 2025; Received in revised form 7 April 2025; Accepted 8 April 2025
Available online 9 April 2025

interface in MMCs introduces additional uncertainty in their plastic deformation processes. Numerous studies have demonstrated that the dimensional features of reinforcements and the interface structure have a strong impact on the dislocations, microcracks, strain/stress and fracture behavior, making accurate theoretical predictions difficult [6–8]. Consequently, the precise processing and delicate design have been severely limited for MMCs.

In recent decades, various explorations have been attempted to achieve a harmonious combination of strength and ductility in MMCs via dispersion technology, interfacial modification and distribution of reinforcements [9–11]. As for the 0D-particle reinforcements, spontaneous agglomeration occurs primarily due to the strong van der Waals forces, particularly in a case where the particle size reaches the nanometer scale or the content in the matrix exceeds a specific threshold (~6 vol%) [12]. Strategies such as nanoparticle self-stabilization, pre-stirring powders in liquid and molecular-level mixing have been proposed to overcome the conundrums in aggregation of reinforcements via overcoming the van der Waals attraction [13,14]. Due to the high aspect ratio of 1D fibers or whiskers, large wetting angles between reinforcements and metal matrix often result in poor interfacial bonding and premature failure under load. Thus, the construction of a semi-coherent/coherent interface in MMCs serves as an effective approach to augment the strength and plasticity of composites by bolstering the bonding strength between reinforcements and metal matrix [15]. Additionally, the popular trend of designing alignment or lamellar structure for 2D nanoplates or nanosheets in metallic matrices has significantly advanced high-performance MMCs, highlighting the importance of configuration design in the matrix [16]. In contrast to the strategies for achieving non-uniform distribution in metals [17], recent works focused on the continuity of the nanoscale reinforcements, that is, the construction of continuous network structure by welding 2D materials or *in situ* growth method. This has been proved to be effective in improving the overall properties of MMCs and opens new avenues for understanding the strengthening and toughing mechanisms [16].

From the above discussion, it can be seen that the strengthening and toughening strategies used for nanoscale reinforcements of different dimensions are usually different. Nowadays, thanks to the development of advanced preparation processes, the integrated properties of nanomaterials have been greatly enhanced, providing a wider range of possibilities in the choice of reinforcements, such as 1D carbon/boron nanotubes or metal nanowires, 2D graphene (GN) or MXene nanosheets and 3D GN networks [18,19]. For example, 1D isolated TiB/Ti achieves extraordinary strength and ductility synergistic enhancement via excellent hetero-deformation-induced (HDI) hardening [20], 2D laminated GN/Cu composites exhibit unique dislocation behavior and crack growth rules by inserting oxygen-containing functional groups at different concentrations on the GN surface [21], and 3D network GN/Cu achieves the balance of strength, plasticity, electronic conductivity, and thermal conductivity because of continuous GN network [22]. In order to fully exploit the advantages of their dimensional feature, it is imperative to systematically investigate and summarize their strengthening and deformation mechanisms, which facilitates the design of MMCs with exceptional comprehensive performances encompassing strength-ductility and other functional properties.

Up to date, some reviews have been dedicated to summarizing the fabrication methods for MMCs reinforced by nanomaterials of varying dimensions [3,5]. However, the existing literature has not sufficiently elucidated the design principles and optimization conditions associated with different reinforcement dimensions, which hinders the accurate prediction of the overall properties in MMCs. Furthermore, the densification and component manufacturing of MMCs are intricately linked to the plastic deformation process. To achieve a synergistic combination of strength and toughness in these materials, it is essential to comprehend the interaction laws between the nanoscale reinforcement and the matrix at both microscopic and macroscopic scales. This review categorized nanoscale reinforcements into 0D, 1D, 2D, and 3D based on their distinct strengthening and toughening mechanisms, as well as the deformation behavior observed in MMCs, as illustrated in Fig. 1. It emphasizes the importance of considering reinforcement dimensions in regulating mechanical properties and understanding the underlying mechanisms. The second to sixth sections of this review independently explore the influential factors and intrinsic mechanisms substantiated by current experimental and theoretical research on the four different dimensional reinforcements. Lastly, this review presents conclusions by providing strategies for selecting the appropriate design of MMCs reinforced by reinforcement with different dimensional features to meet usage requirements and optimize structural performance more elegantly.

2. Metal matrix composites reinforced with 0D reinforcements

Being first introduced into metals in the 1970s and 1980s [23,24], the utilization of 0D reinforcements in MMCs is widespread owing to their exceptional strength and modulus [25,26]. However, the agglomeration tendency of ceramic particles and their poor wettability with metal matrix often pose challenges in achieving effective dispersion and interface bonding between reinforcement particles and matrix. Therefore, the dispersion of ceramic particles in MMCs and the enhancement of interface bonding between them have consistently been the focal points and challenges of research. In response to the above situation, researchers have made numerous attempts, as depicted in Fig. 2, which are manifested in three aspects: new techniques for achieving the uniform dispersion of reinforcements, the design of interface composition and structure, and the special non-uniform distribution of reinforcements. For the uniform dispersion of 0D reinforcements in MMCs, researchers employed some methods such as friction stir processing [27], ball milling [28], nanoparticle self-stabilization [14] and electromagnetically induced acoustic cavitation [29] to achieve reinforcements uniform dispersion within the metal, enhancing stress distribution by preventing agglomeration and mitigating early failure of the MMCs caused by stress concentration. In terms of the reinforcements/metal interface design, previous research was primarily focused on improving interface bonding through the formation of semi-coherent/coherent interfaces [30], introducing interphases [31], and establishing core-shell reinforcement [32] to prevent premature fracture resulting from interface debonding

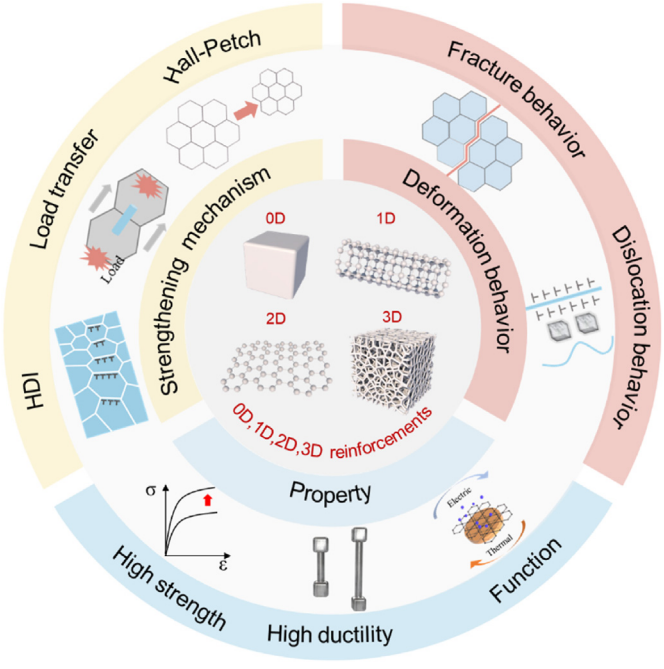

Fig. 1. Overview of MMCs reinforced with various dimensional reinforcements, focusing on properties, strengthening mechanisms and deformation behavior.

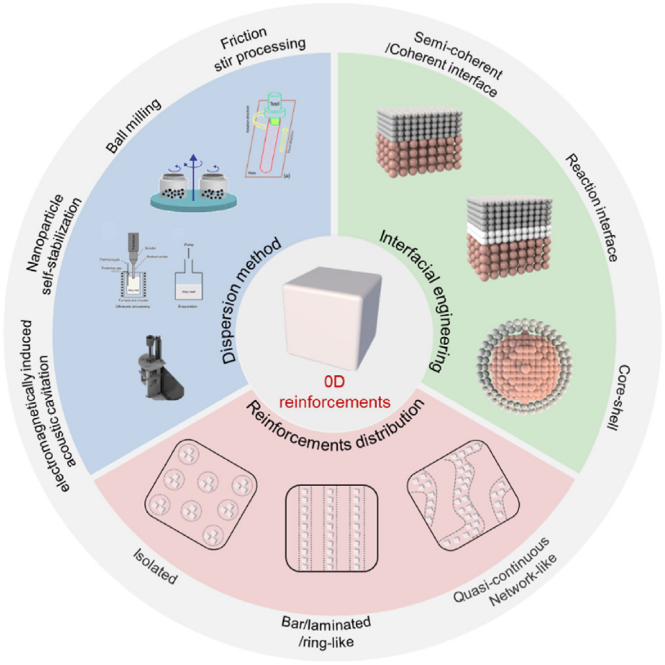

Fig. 2. Overview of the strategies for achieving exceptional properties in MMCs reinforced with 0D reinforcements. Taken from Refs. [14,27–29] with permissions.

during loading. For the non-uniform distribution of reinforcements, researchers have utilized isolated reinforcement [10], bar and laminated/ring-like reinforcement [33] and quasi-continuous network--like (QCNL) reinforcement [34,35] to induce a non-uniform distribution of reinforcements within MMCs. This introduction of non-uniformity further regulates strengthening and toughening mechanisms as well as plastic deformation behavior of MMCs, ultimately improving both strength and plasticity.

In this section, the dispersion process, interface design and distribution of 0D reinforcements are discussed, systematically summarizing the comprehensive properties of MMCs under different strengthening strategies.

2.1. Dispersion and interface design of 0D reinforcements

The size effect of 0D reinforcements and the bonding strength of reinforcements/metal interface play crucial roles in determining the comprehensive properties of MMCs, as well as serving as the pivotal factors in overcoming the strength and ductility trade-off. Traditional composites reinforced with micron-sized particles often exhibit weak interactions with dislocations and may fracture prematurely due to the stress concentration around particles. In contrast, dislocations cannot cut but only bypass nanoscale particles in MMCs, resulting in strong pinning of dislocation and additional work hardening [36]. However, nanoscale particles tend to agglomerate due to their high surface energy, which diminishes their enhancement effect. In addition, the hard and brittle nature of 0D reinforcements, along with their limited wettability with metals, leads to premature brittle fractures in MMCs, significantly affecting their engineering applications. Consequently, it remains a tough task to synthesize uniformly distributed nano 0D reinforcements in the metal matrix. Li et al. [28] reported the uniform dispersion of ultra-fine carbon nanoparticles (~2.6 nm) in Cu matrix (nc-Cu), and realized the synergistic improvement of strength and plasticity by using a chemical bond-assisted dispersion strategy (Fig. 3a). This synergistic enhancement is attributed to the incorporation of uniformly dispersed ultra-fine carbon nanoparticles into the matrix. Firstly, the presence of nanoparticles exerts a significant stabilizing effect on dislocations and enhances work hardening. Secondly, the inclusion of nanoparticles also triggers multiple slips within grains, thereby providing additional strengthening through back stress and work hardening. Additionally, Chen et al. [14] successfully achieved the homogeneous dispersion of SiC particles with a large volume fraction (14 vol%) into the magnesium matrix. This is accomplished by overcoming the van der Waals barrier of SiC agglomeration through thermal activation during the heating process (Fig. 3b). The high density of SiC nanoparticles impedes dislocation slip along the basal plane of magnesium matrix, and may also potentially trigger slip on other crystallographic planes during deformation.

Furthermore, achieving uniform dispersion of ceramic particles becomes increasingly difficult as their size decreases. For ceramic particles smaller than 10 nm, this challenge becomes a significant issue for MMCs. Bai et al. [11] introduced an “interface replacement” strategy aimed at enhancing the dispersion of ceramic nanoparticles into metals thus achieving extraordinary mechanical properties. This approach involves substituting the strongly bonded interface between ceramic nanoparticles with a weakly connected van der Waals force between few-layer GN-like layers. By implementing this method, they achieved a dense and uniform dispersion of approximately 5 nm MgO particles which exhibited a fully coherent MgO/Al interface. The coherent MgO/Al interface increases the activation energy of vacancy dramatically, thereby reducing the likelihood of fractures along the interface. Meanwhile, the very small coherent MgO particles, with 5 nm in size, lead to high Zener pinning of grain boundaries. As a result, the composite demonstrates unprecedented strength (~200 MPa) and creep resistance at 500 °C (Fig. 3c). This work also highlights the role of interfaces in achieving optimal mechanical properties at both room and high temperatures.

2.2. Non-uniform distribution of 0D reinforcements

Despite of extensive research having been conducted on optimizing the size, dispersion, and interface state of 0D reinforcement in MMCs, the bulk composites with nanoscale, dense and uniform dispersion in MMCs usually show a low ductility or fracture toughness due to the difficulty for dislocation gliding within the metal matrix. Recently, researchers have made impressive progress by designing the non-uniform distribution of 0D reinforcements within MMCs to tackle the aforementioned problem. As shown in Fig. 4, these breakthroughs in the strength and plasticity trade-off are attributed to the expanded plastic deformation zones of particles in the metal matrix by superposing the zones of a single particle. For example, Jiang et al. [10] prepared B_4C reinforced aluminum matrix composites with an inhomogeneous reinforcement distribution through a meticulously designed ball milling process. This innovative approach results in a 26 % increase in tensile strength and a 30 % increase in toughness compared to composites reinforced by uniformly distributed B_4C particles. Specifically, the aluminum matrix in these composites can be divided into two distinct zones: nanoparticle-rich (NPR) zones and nanoparticle-free (NPF) zones. The NPR zones act as a “hard phase”, while the NPF zones function as a “soft phase” (Fig. 4a and 5a). During deformation, the hard phase primarily bears the load transfer, whereas the soft phase facilitates the plastic deformation through dislocation behavior. This inhomogeneous distribution of hard and soft phases induces non-uniform deformation, which in turn provides additional strength through back stress. Furthermore, the uneven distribution of B_4C within the matrix leads to the overlapping of dislocation punched zones, thereby reducing crack nucleation around B_4C and enhancing the overall toughness. In addition, other works reported by Sun et al. [33] and Huo et al. [34] also prepared laminated Al_2O_3/Al and QCNL (TiC + Ti_5Si_3)/Ti composites, in which systems the synergistic increase of strength and ductility due to the coordinated deformation between soft and hard phases were realized (Fig. 4b–d). In conclusion, the properties of the composite are significantly influenced by the ratio of hard and soft phases. Generally, an increased proportion of hard phases results in higher strength. However, there are considerable challenges associated with the preparation of composites containing a high content of hard

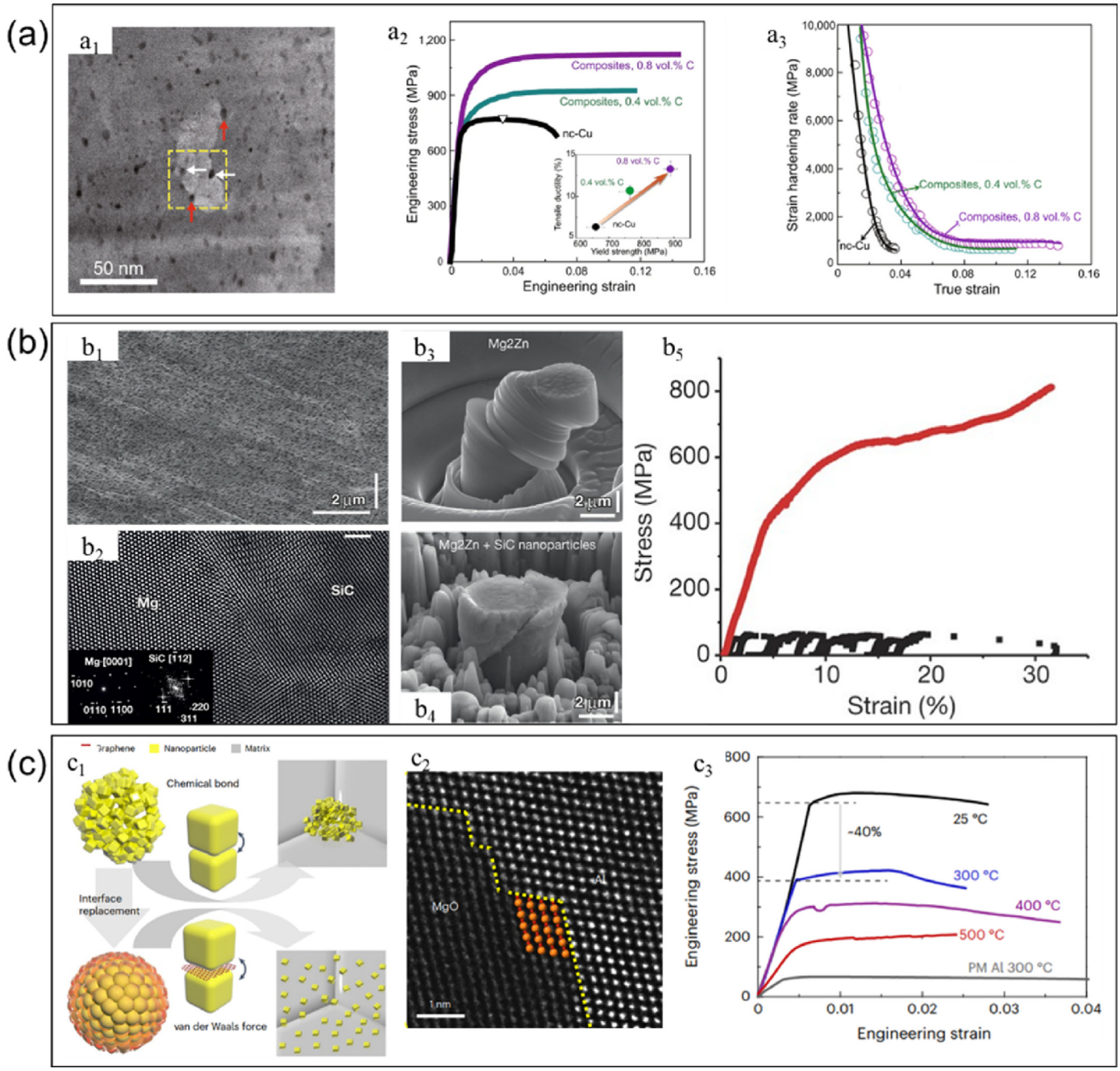

Fig. 3. Microstructure and properties of MMCs reinforced with 0D reinforcements. (a) nc-Cu. a_1: STEM image of nanocarbon particles; a_2: stress-strain curves for pure Cu and nc-Cu composites; a_3: strain hardening rate for pure Cu and nc-Cu composites [28]. Taken from Ref. [28] with permission. (b) SiC/Mg. b_1: the uniform dispersion and dispersion of SiC; b_2: a characteristic interface between SiC and matrix; b_3 and b_4: the morphology of post-deformed samples without and with SiC; b_5: engineering stress-strain curves of micropillar as-solidified samples without and with (red) SiC [14]. Taken from Ref. [14] with permission. (c) MgO/Al. c_1: schematic diagram of the interface-replacement dispersion process of MgO NPs; c_2: HRTEM image of MgO/Al interface; c_3: tensile engineering stress-strain curves of as-extruded MgO@GL/Al and Al [11]. Taken from Ref. [11] with permission.

phase. Luo et al. [37] observed the QCNL of SiC particles, as shown in Fig. 4c and 5c, within the magnesium matrix through ball milling, resulting in the formation of an inverse nacre structure. The authors proposed that the pure Mg sheet embedded in the continuous Mg matrix composite reinforced with SiC particles can accommodate a great amount of hard phase. The heterogeneous deformation of the soft and hard phases results in HDI strengthening, thereby providing an additional strengthening mechanism. Moreover, the strain hardening of the soft phase compensates for the strength reduction caused by micro-crack formation within the matrix, which prevents softening in composites under strain and consequently achieves higher elongation compared to the composites with homogenous reinforcement distribution.

In summary, the primary strengthening mechanisms attributed to the non-uniform distribution of 0D reinforcements are generally associated with HDI hardening, which arises from the non-uniform deformation of the soft and hard phases during deformation. Additionally, the primary toughening and plastic deformation mechanisms include crack nucleation and reduction in NPR region caused by the overlapping of dislocation punched zones, as well as the deflection of cracks at the NPR/NPF interface (Fig. 5). These points will be further elaborated in Section 6.

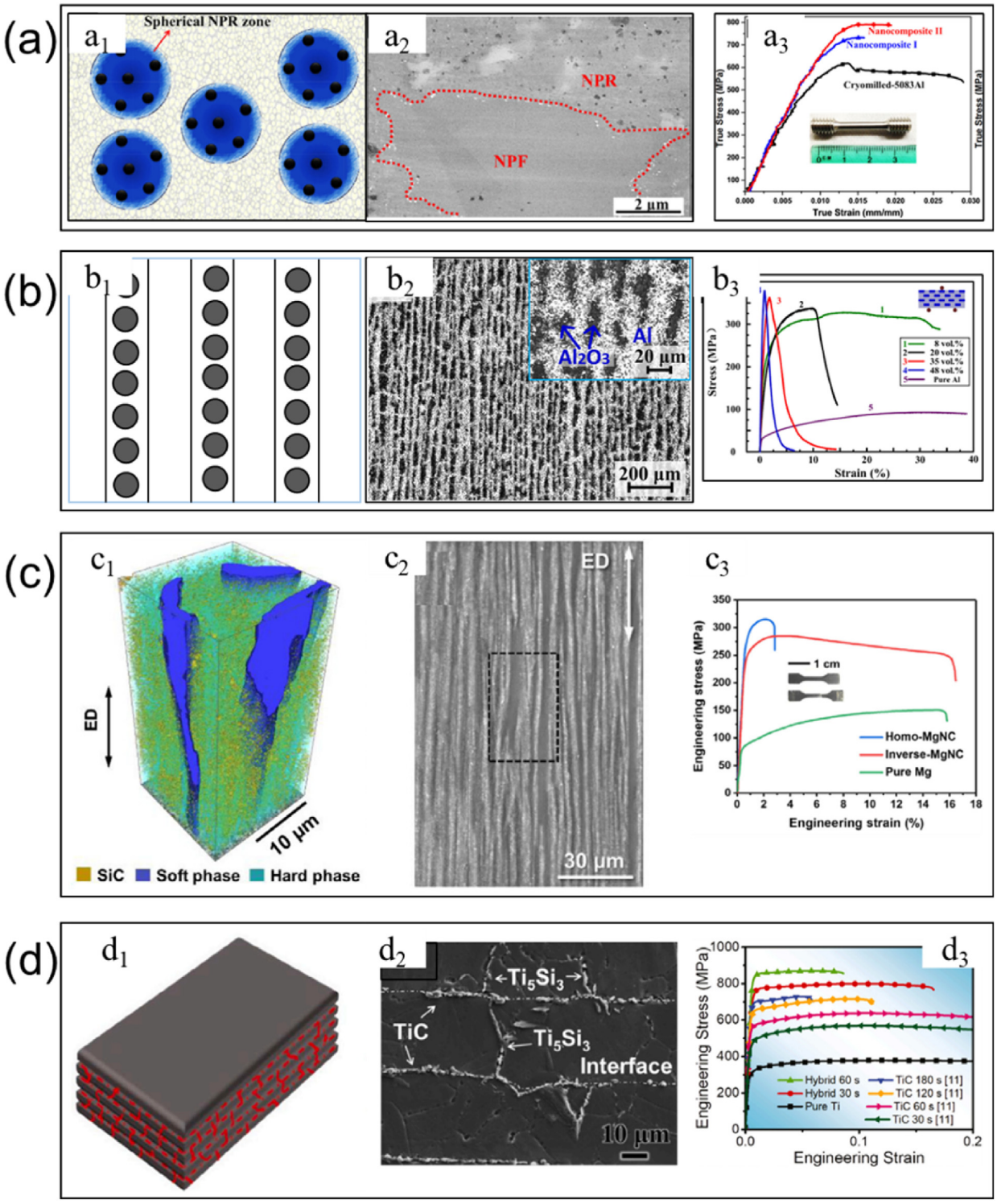

Fig. 4. Microstructure and properties of MMCs reinforced with the non-uniform distribution of 0D reinforcements. (a) Isolated B_4C/Al. a_1: schematic illustration; a_2: SEM image of B_4C/Al; a_3: tensile true stress-strain curves of composites [10]. Taken from Ref. [10] with permission. (b) Bar/laminated/ring-like Al_2O_3/Al. b_1: schematic illustration; b_2: SEM image of Al_2O_3/Al; b_3: three-point bending stress-strain curves of Al_2O_3/Al [33]. Taken from Ref. [33] with permission. (c) QCNL SiC/Al. c_1: schematic illustration; c_2: SEM image of SiC/Al; c_3: tensile engineering stress-strain curves of SiC/Al [37]. Taken from Ref. [37] with permission. (d) QCNL TiC-Ti_5Si_3/Ti. d_1: schematic illustration; d_2: SEM image of TiC-Ti_5Si_3/Ti; d_3: tensile engineering stress-strain curves of TiC-Ti_5Si_3/Ti [34]. Taken from Ref. [34] with permission.

2.3. Summary of the attainable mechanical properties of MMCs reinforced with 0D reinforcements

The normalized tensile strength and elongation of MMCs reinforced with 0D reinforcements, as reported in the literature, are illustrated in Fig. 6. The non-uniform distribution of these 0D reinforcements significantly influences the correlation between the strength and elongation of MMCs. Compared to homogeneous MMCs, heterogeneous composites exhibit not only a pronounced strengthening effect but also considerable plasticity and toughness, even approaching or surpassing the elongation

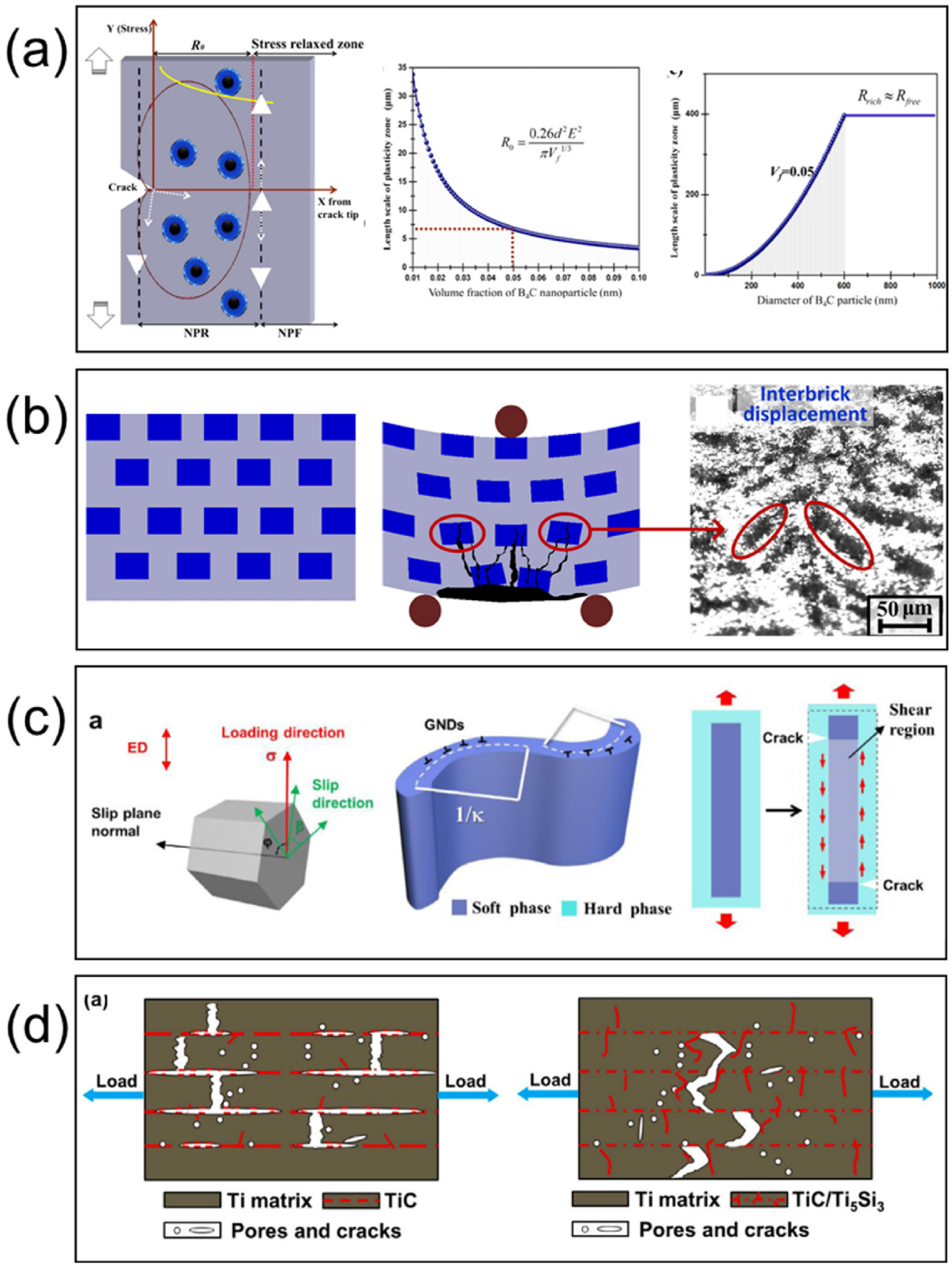

Fig. 5. Schematic illustration of strengthening and fracture mechanism of MMCs reinforced with the non-uniform distribution of 0D reinforcements: (a) Isolated [10]. (b) Bar/laminated/ring-like [33]. (c, d) QCNL, c [37]: and d: [34]. Taken from Refs. [10,33,34,37] with permissions.

of the metal matrix. Consequently, utilizing MMCs reinforced with heterogeneous 0D reinforcements offers an effective strategy to overcome the limitations imposed by the trade-off between strength and plasticity.

3. Metal matrix composites reinforced with 1D reinforcements

In recent decades, significant advancements and remarkable achievements have been made in the study of 0D reinforcements reinforced MMCs. However, with the rise of emerging industries like

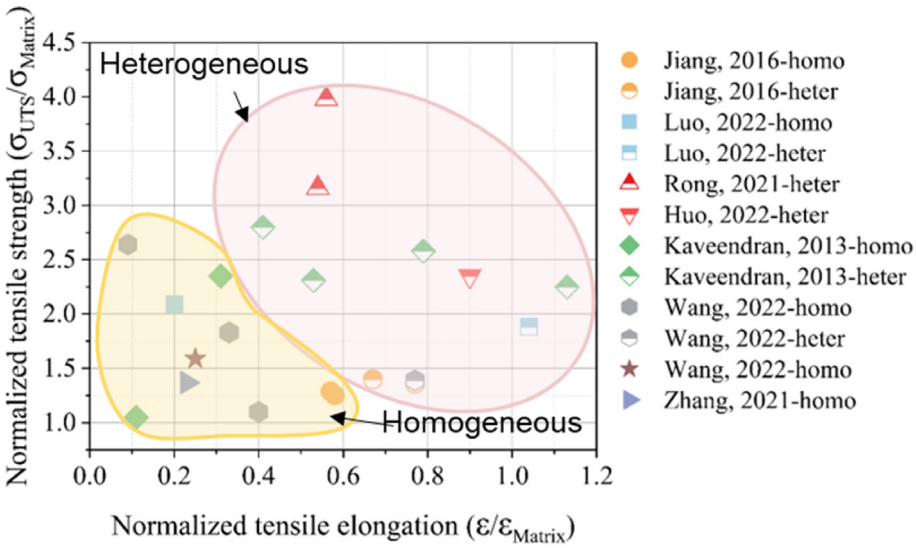

Fig. 6. Maps of normalized tensile strength versus normalized tensile elongation of MMCs reinforced with 0D reinforcements [10,32,34,38–42].

integrated circuits and new energy vehicles, there is a growing demand for functional properties such as electrical and thermal conductivity in MMCs. Therefore, some researchers have shifted their focus to MMCs reinforced with 1D nanomaterials that are characterized by a large length/diameter ratio [43]. The 1D reinforcements in MMCs consist of carbon nanotubes (CNTs) and ceramic whiskers, known for their outstanding strength, hardness, high-temperature thermal stability, and electrical and thermal conductivity, making them ideal for enhancing the properties of MMCs. Generally, achieving the uniform dispersion of CNTs within the metal matrix is a difficult task due to the interwinding nature and agglomeration tendencies of flexible CNTs, while poor wettability prevents whiskers from having a tight interface with the metal matrix considering their high stiffness and inert side walls [44]. Therefore, achieving an outstanding strengthening effect requires good control of both structural integrity and dispersion of 1D reinforcements simultaneously. The current state of research has prompted researchers to undertake many endeavors, as depicted in Fig. 7, encompassing four primary aspects: (1) Dispersion method. Various dispersion processes are proposed to address the dispersion of 1D reinforcements in MMCs, including liquid-assisted mixing [45], ball milling [46] and ultrasonic-assisted melting method [47]. Among these methods, ball milling stands out as the most commonly used due to its simplicity and efficiency. (2) Characteristic parameters. The dispersion type [48] (grain boundaries and territories) and the feature size [49] are considered as two most important factors that influence the strengthening effects. The large aspect ratio of 1D reinforcements introduces unique interaction mechanisms with dislocations in MMCs. It consequently leads to varying strengthening and toughening mechanisms, as well as plastic deformation behavior within MMCs. (3) Non-uniform distribution of reinforcements. The strategically designed non-uniform distribution of

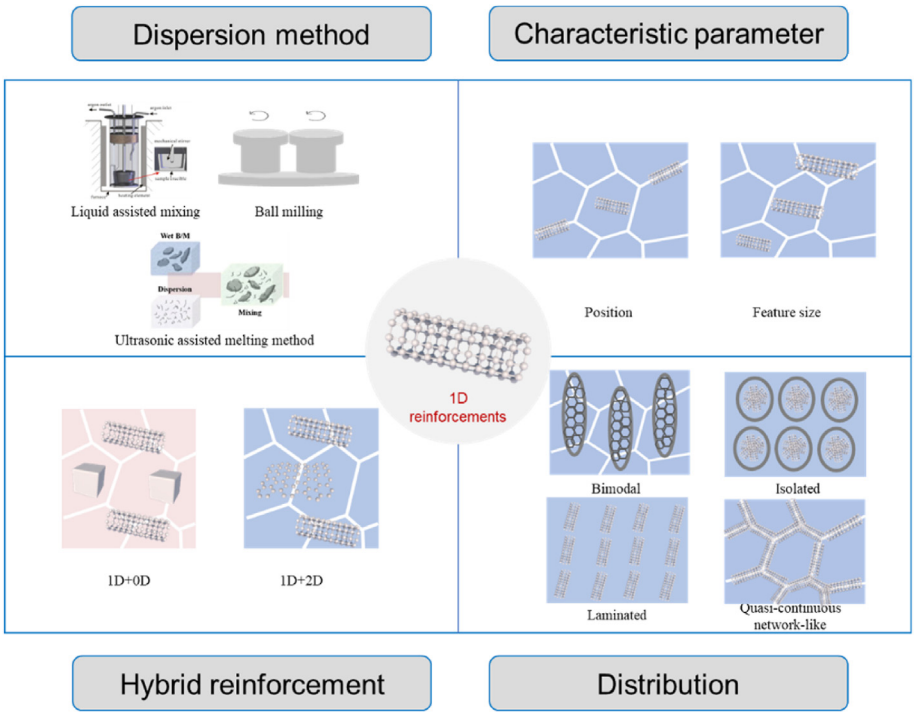

Fig. 7. Overview of MMCs reinforced with 1D reinforcements. Taken from Refs. [45,47] with permissions.

reinforcements, including bimodal grain structure [50], isolated reinforcements [20], laminated-like reinforcements [51,52], and QCNL reinforcements [53,54] will be introduced systematically. (4) Hybrid reinforcement. The delicately designed 0D-*x*D ($x = 1$ or 2) hybrid reinforcements have been proposed to achieve the synergistic effect in strengthening and toughening [55,56].

This section discusses the four primary aspects of the design and fabrication of MMCs reinforced by 1D reinforcements, followed by clarifying the comprehensive understanding of 1D reinforcement and its impact on the mechanical properties of MMCs.

3.1. Characteristic parameter of 1D reinforcements

The aspect ratio of the 1D reinforcements has a significant influence on their dispersion state within the matrix. Typically, the 1D reinforcements with a high aspect ratio are predominantly located at grain boundaries, while those with a small aspect ratio tend to distribute within the grains. Studies have shown that ball milling is effective in achieving intragranular dispersion of CNTs. The incorporation of 1D reinforcements within matrix grains plays a crucial role in grain refinement and dislocation hindrance, contributing to the overall enhancement of MMCs. Xu et al. [48] employed the flake powder metallurgy technique to fabricate composites of CNTs/Al, in which the influence of characteristic parameters of CNTs on the mechanical strength and plasticity was clarified (Fig. 8a). These parameters include grain size, volume fraction, dispersion type, aspect ratio, and interface reaction rate. The authors conclude that the influence of CNTs distributed at grain boundaries on the strength and plasticity of composite is less correlated to the aspect ratio of CNTs. On the contrary, for the CNTs distributed within grains, the ultimate tensile strength and uniform elongation of the composite primarily rely on the aspect ratio. Smaller aspect ratios of CNTs often result in improved comprehensive properties of composite because of the difficult movement for mobile dislocations within grains. In order to further investigate the influence of the aspect ratios of CNTs on the strengthening mechanisms of composite, Chen et al. [49] utilized powder metallurgy to fabricate three composite materials with varying aspect ratios. They found that adjusting the aspect ratios of CNTs could customize the strength of composites, including modulation of the strengthening mechanisms accordingly. Specifically, CNTs with aspect ratios above 40 mainly reinforced the composites through load transfer strengthening, while those with aspect ratios below 10 are primarily strengthened by the Orowan mechanism (Fig. 8c). In addition, the orientation of 1D reinforcements significantly affect its strengthening effect in MMCs. The off-axis angle (θ in Fig. 8b), as defined by Le et al. [57], introduced a universal shear-lag model that accurately evaluated the load transfer strength in all composites regardless of matrix and reinforcements. The results indicate that the strengthening effect of 1D reinforcements diminishes as the off-axis angle increases. Therefore, the aspect ratio, dispersion type, and orientation of 1D reinforcements must be carefully considered in the design of MMCs to achieve optimal strengthening effects and exceptional overall performance.

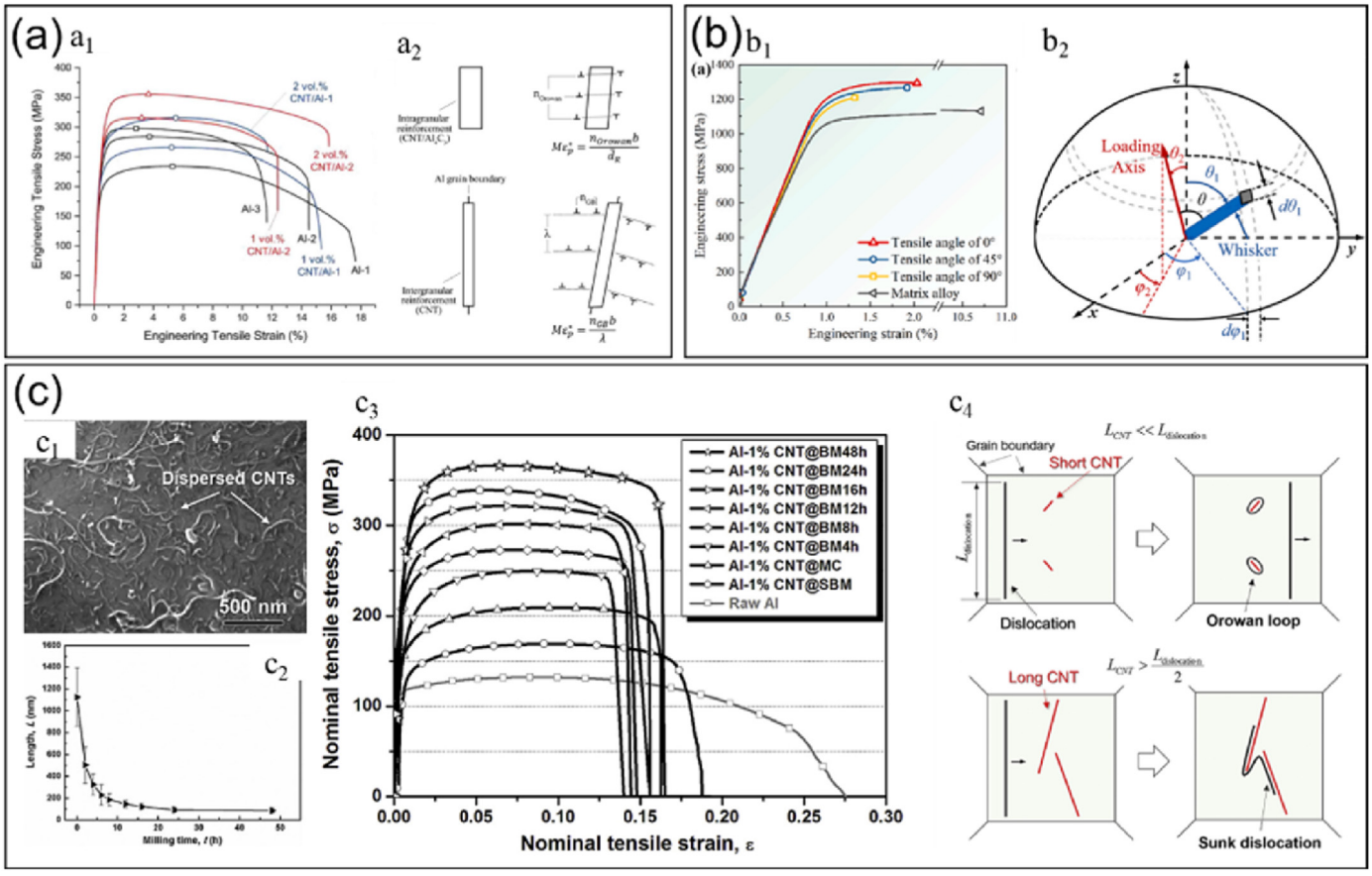

Fig. 8. Properties and mechanisms of MMCs reinforced with 1D reinforcements based on position, orientation and size. (a) Reinforcements position. a_1: engineering stress-strain curves of the CNTs/Al composites; a_2: schematic illustration of dislocation behavior with CNTs in intragranular and intergranular [48]. (b) Reinforcements orientation. b_1: engineering stress-strain curve of matrix alloy and TiB/Ti composite at different tensile angles; b_2: definition of the spatial orientation of whiskers and applied stress [57]. (c) Reinforcements size. c_1: SEM image of the CNTs; c_2: the relationship between the time of ball milling and CNTs size; c_3: engineering stress-strain curves of the CNTs/Al composites; c_4: schematic illustration of dislocation behavior with CNTs among the size [49]. Taken from Refs. [48,49,57] with permissions.

3.2. Non-uniform distribution of 1D reinforcements

The 1D reinforcements, with their larger length/diameter ratio, exhibit anisotropic properties and influences on the matrix, compared to 0D reinforcements. Considering these characteristics, it is crucial to conduct spatial non-uniform distribution of reinforcements in order to fully utilize the strength and toughness of 1D reinforcements. In general, the non-uniform distribution of reinforcements in MMCs can be approached by considering two aspects: altering the grain non-uniform distribution of the matrix and regulating the non-uniform distribution of reinforcement, as highlighted in Fig. 9. Taking steps along the first path, Ma et al. [58] designed a heterogeneous grain structure in CNTs reinforced aluminum matrix composites, achieving a high tensile strength of 720 ± 6 MPa and elongation of 4.7 ± 0.5 % (Fig. 9a). The heterogeneous grain structure design results in the formation of ductility and brittle zones, which reduces stress localization in the ductility zone and mitigates stress concentration at grain boundaries and interfaces between ductility and brittle zones. The key to achieving cooperative enhancement of strength and ductility in MMCs through grain structure design lies in the effective regulation of both coarse-grained and fine-grained regions. In other words, the grain structure design is accomplished by manipulating the spatial non-uniform distribution of 1D reinforcements to influence the grain structure. Therefore, the non-uniform distribution of 1D reinforcements allows for more precise control over the coarse-grained and fine-grained regions. A good example is that titanium matrix composites reinforced with isolated TiBw (TiB--whisker) [20], which achieved an excellent balance between the UTS of 1065 ± 25 MPa and fracture elongation of 12.0 ± 0.48 %, while 961 ± 34 MPa and 3.6 ± 0.31 % for homo-structured composite (Fig. 9b). The authors suggested that the synergistic improving primarily from the HDI hardening is caused by non-uniform deformation because of isolated TiBw. Additionally, the unique design of the isolated TiBw plays a crucial role in enhancing both strength and toughness by providing isotropic deformability and a high capacity for dislocation storage. In addition, the non-uniform distribution of reinforcements in MMCs has the potential to enhance both strength and ductility by exerting influence on the texture

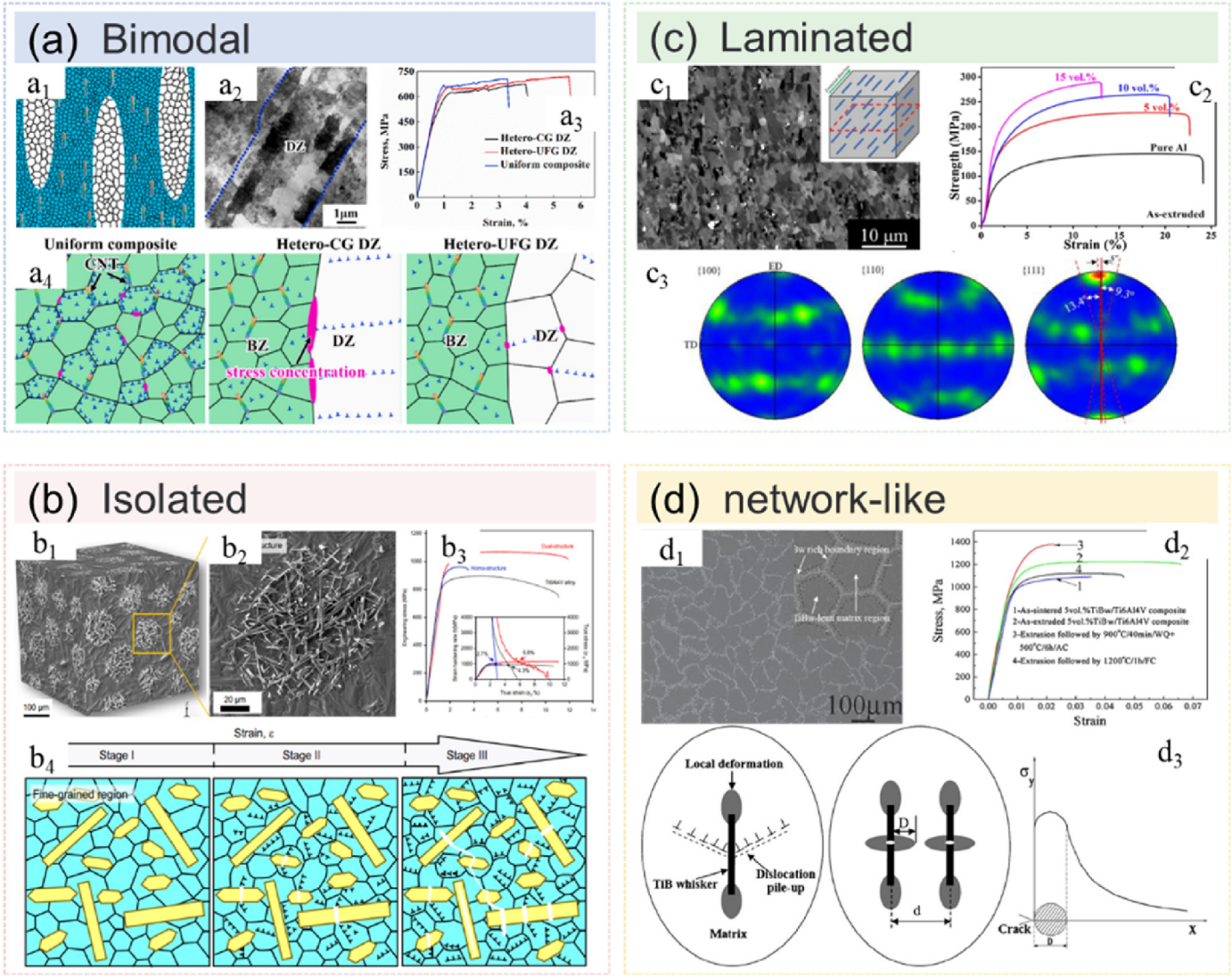

Fig. 9. Microstructure, properties and mechanism of MMCs reinforced with the non-uniform distribution of 1D reinforcements. (a) Bimodal distribution. a_1: schematic illustration; a_2: microstructure image of CNT/Al; a_3: stress-strain curves of uniform and heterogeneous composites; a_4: schematic illustration of deformation behavior and damage mechanism of composites [58]. (b) Isolated. b_1: schematic illustration; b_2: microstructure image of TiB/Ti6Al4V; b_3: stress-strain curves of dual structure, homo structure and Ti6Al4V alloy; b_4: schematic illustration of dislocation behavior during deformation [20]. (c) Laminated: c_1: schematic illustration and microstructure image of laminated; c_2: stress-strain curves of Si_3N_4w/Al; c_3: pole figures of Si_3N_4w/Al composites [51]. (d) QCNL. d_1: schematic illustration and microstructure image of laminated. d_2: stress-strain curves of TiB/Ti64; d_3: schematic illustrations of stress distribution [53]. Taken from Refs. [20,51,53,58] with permissions.

evolution during deformation. Zhang et al. [51] constructed Si_3N_4w/Al composite with a laminated-like design using hot extrusion (Fig. 9c). The authors emphasized the critical role of creating a strong Si_3N_4w/Al interface and textures in achieving simultaneous improvements in strength and plasticity. They revealed that the formation of an isolated Si_3N_4w design during hot extrusion is advantageous for enhancing the interface bonding between the Si_3N_4w and Al matrix, as well as for facilitating the formation of <111> and <100> textures. Furthermore, the TiBw/Ti composites reinforced with QCNL reinforcement were fabricated by Huang et al. [53] using a customized powder metallurgy process and hot extrusion technique, to fabricate TiBw/Ti composites, resulting in notable improvements in strength, plasticity, and modulus. The authors argued that the observed increase in heightened strength can be attributed to grain refinement because of the QCNL TiBw. In addition, the introduction of the QCNL also results in a transformation of the plastic deformation behavior of the matrix. Stress is confirmed to concentrate preferentially near TiBw during the deformation process, leading to their fracture rather than pull-out. Simultaneously, on a larger scale, TiBw can be multiple-fractured or even repeatedly fractured to bear higher loads due to the overlapping of plastic deformation caused by the QCNL TiBw. Therefore, the network-like distribution is advantageous in effectively regulating the stress state and crack behavior of the matrix, facilitating improvements in plasticity and toughness.

3.3. Hybrid reinforcements

On the one hand, incorporating 1D reinforcements such as CNTs or whiskers with higher aspect ratios is advantageous for achieving enhanced load transfer. On the other hand, this also imposes limitations on its ability to strengthen in the direction perpendicular to the axis. In recent years, researchers have effectively addressed the aforementioned issues by incorporating hybrid reinforcements, harnessing the inherent advantages of different dimensional reinforcements [59]. Shan et al. [60] prepared a hybrid reinforced CNTs@Al_2O_3/Al composite through an *in situ* reaction, as shown in Fig. 10a. H_3BO_3, in combination with the oxygen-containing functional groups on the outer surface of CNTs, synthesizes Al_2O_3 in the subsequent *in situ* reaction, increasing the axial contact area between CNTs and the matrix. The dispersion of Al_2O_3 particles led to grain refinement, while the formation of CNTs@Al_2O_3 hybrid reinforcements contributed to improved interface bonding between CNTs and matrix, thereby facilitating the improved load transfer strengthening. From another aspect, during the deformation process, cracks tend to concentrate near the CNTs@Al_2O_3 hybrid reinforcements rather than the CNTs/Al interface, suggesting the ability of Al_2O_3 particles to impede dislocation movement and dissipate crack propagation energy. Additionally, the presence of Al_2O_3 enhanced interfacial shear force and hindered premature material failure due to CNTs pulling out, highlighting the beneficial effect of hybrid reinforcements in exceeding the performance of composites reinforced by single-type reinforcements. Zhang et al. [55] reported the study in which they employed an *in situ* space-confined synthesis method hybrid to prepare a CNTs-GN hybrid reinforced Cu matrix composite and obtained excellent matching of strength and plasticity, as shown in Fig. 10b. They reckon that the exceptional alignment of CNTs confined in the *in situ* synthesized GN layers benefited to the ductility and toughness of the composites. The incorporation of GN in the composite serves a dual role: Firstly, it contributes to the uniform dispersion of CNTs thus refining the grains. Secondly, the large aspect ratio of GN improves the interfacial binding of CNTs to the matrix, thereby enhancing load transfer strengthening. Furthermore, the CNTs-GN hybrid reinforcement has also revealed a deflection effect on the relative crack during deformation, which is beneficial for improving extrinsic toughening.

3.4. Summary of the attainable mechanical properties of MMCs reinforced with 1D reinforcements

The relationship between aspect ratio versus normalized strength and elongation, content of 1D reinforcements versus normalized strength, and normalized strength versus elongation of MMCs reinforced with 1D reinforcements are summarized in Fig. 11. As illustrated in

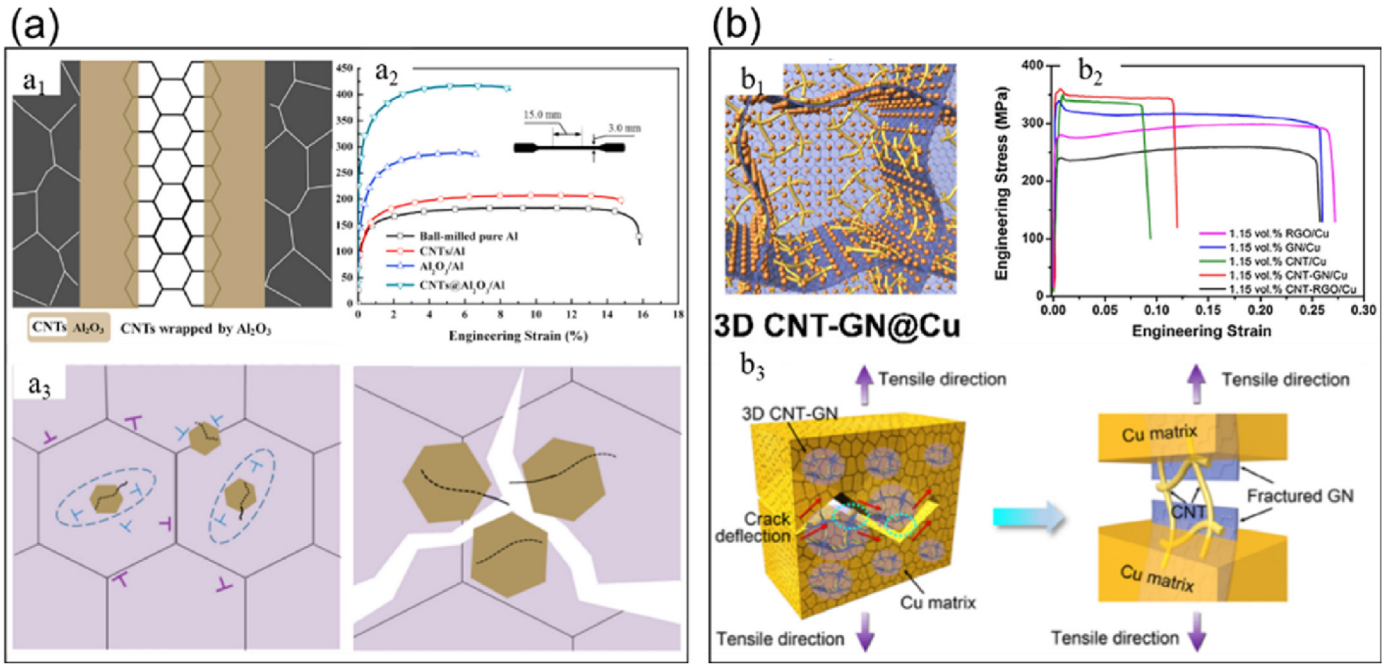

Fig. 10. Properties and mechanism of MMCs reinforced with hybrid reinforcements. (a) 1D+0D. a_1: schematic illustrations of interfacial coupling profile. a_2: tensile stress-strain of pure Al, CNTs/Al, Al_2O_3/Al and CNTs@Al_2O_3/Al composites. a_3: schematic illustrations of fracture mechanism [60]. (b) 1D+2D. b_1: schematic depiction of the model simplification of the hybrid reinforcements. b_2: stress-strain curves of Cu matrix composites reinforced by RGO, GN, CNTs, CNTs-GN and CNTs-RGO. b_3: schematic illustration showing crack deflection of CNTs-GN in the path of fracture and a close-up of the pull-out bridging of CNTs during tensile deformation [55]. Taken from Refs. [55,60] with permissions.

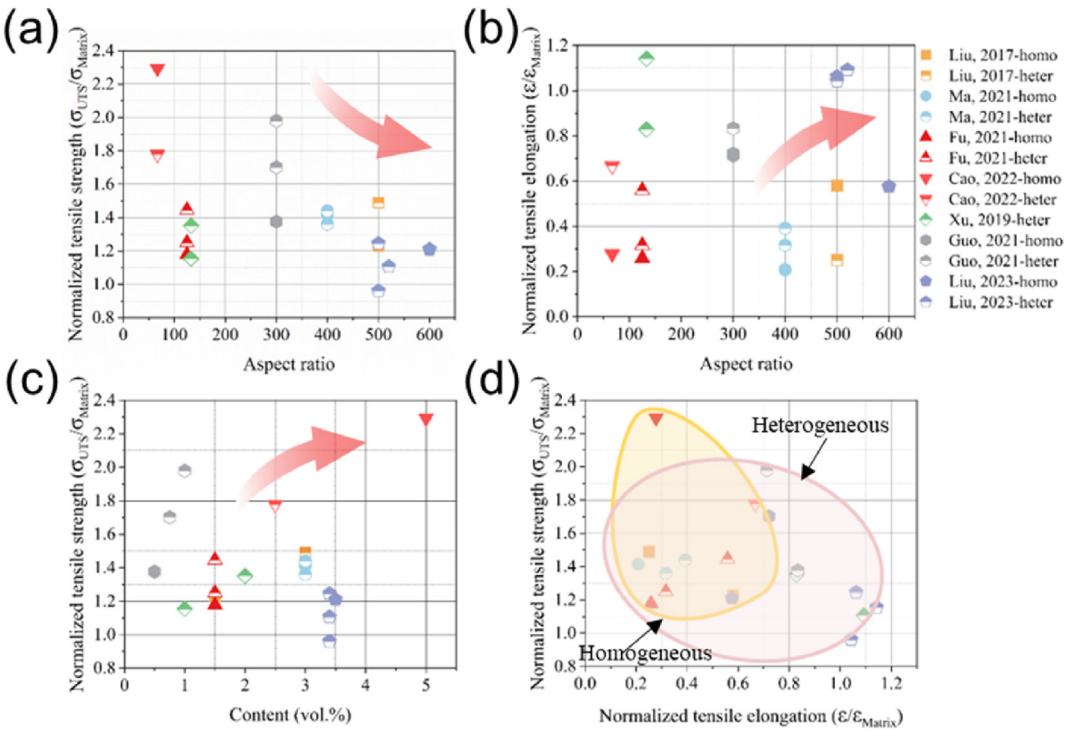

Fig. 11. Maps of (a) normalized tensile strength versus aspect ratio of 1D reinforcements, (b) normalized tensile elongation versus aspect ratio of 1D reinforcements, (c) normalized tensile strength versus content of 1D reinforcements and (d) normalized tensile strength versus normalized tensile elongation of MMCs reinforced with 1D reinforcements [20,46,48,50,61–63].

Fig. 11a and b, 1D reinforcements with a low aspect ratio exhibit a pronounced strengthening effect, whereas those with a high aspect ratio demonstrate superior ductility improvement. This phenomenon can be attributed to distinct strengthening mechanisms: 1D reinforcements with a low aspect ratio primarily function as Orowan reinforcement, while those with a high aspect ratio predominantly serve as load transfer reinforcement. The content of 1D reinforcement significantly influences the strengthening effect, with higher content generally resulting in greater strength. The in-depth analysis of the data in Fig. 11a–c reveals that the heterogeneous non-uniform distribution of 1D reinforcements can alter the relationship between aspect ratio, strength and elongation, as well as content and strength to a certain extent. This allows for achieving a harmonious balance between strength, plasticity, and toughness. More intuitive data is plotted in Fig. 11d.

4. Metal matrix composites reinforced with 2D reinforcements

Two-dimensional materials such as GN, boron nitride, transition metal dichalcogenides, black phosphorus, MXenes, and semimetals have attracted huge and widespread interest over the past years for their excellent properties, such as in-plane strength (~150 GPa) and elastic modulus (1000 GPa), unique electrical (10^8 S m^{-1}) and thermal (2000–5000 W m^{-1} K^{-1}) conductivity characteristics and large specific surface area (up to 2630 m^2 g^{-1}) in electronics, optoelectronics, catalysis, energy storage, solar cells, sensors, biomedicine and other fields [64–66]. In recent years, the incorporation of 2D materials into MMCs has surmounted remarkable research outcomes in aerospace, transportation, electronic communications and smart chips owing to their exceptional mechanical and functional properties [1,67]. Furthermore, the 2D reinforcements possess a significantly larger specific surface area compared to 0D reinforcements and 1D reinforcements, thereby introducing quantities of interfaces into the metal matrix. This characteristic facilitates the modulation of the mechanical and functional properties of the composites, which attracts wide interest from researchers [68]. Currently, the development of MMCs reinforced with 2D reinforcements has been hindered by two primary challenges: (1) the defects of 2D reinforcements added in MMCs; (2) the inadequate interface strength between 2D reinforcements and metal matrix. This is because the performance of 2D reinforcements can be significantly degraded due to defects, while weak interface bonding may result in premature material failure during service caused by interface debonding [69,70]. Thus, the current research focuses on how to reduce the defects of 2D reinforcements in MMCs and how to improve the interface strength of 2D reinforcements/metal, as shown in Fig. 12, and can be divided into four parts: (1) Dispersion method. The dispersion of 2D reinforcements in MMCs has been addressed by various dispersion processes proposed, including ball milling [71], *in situ* reaction [72], electro-deposition [73] and molecular mixing [74]. *In situ* reaction represents the optimal approach for preparing 2D reinforcements/MMCs, taking into account the dispersion effect, quality of 2D reinforcements, and process cost. (2) Characteristic parameter. The enhancement effect of 2D reinforcements is related to its feature parameters, such as shape [75], size [76] and quality [77] of 2D reinforcements. (3) Two-dimensional reinforcements/metal interface. Covalent bond [78], interface modification [79] and interface shape design [80] are regarded as viable approaches to enhance interface bonding. (4) Non-uniform distribution of reinforcements. The authors aim to address the tradeoff of strength and toughness in MMCs reinforced with 2D reinforcements by achieving a laminated structure [81].

In this section, the dispersion process, characteristic parameter, 2D reinforcements/metal interface and non-uniform distribution of 2D reinforcements are discussed, and the comprehensive properties of MMCs are systematically summarized by examining the effects of various strategies.

4.1. Characteristics of 2D reinforcements

In contrast to the growth of 2D materials on flat metal and thin films, the 2D reinforcements in MMCs inevitably exhibit certain distinctions that include variations in sheet shape, size, and surface quality,

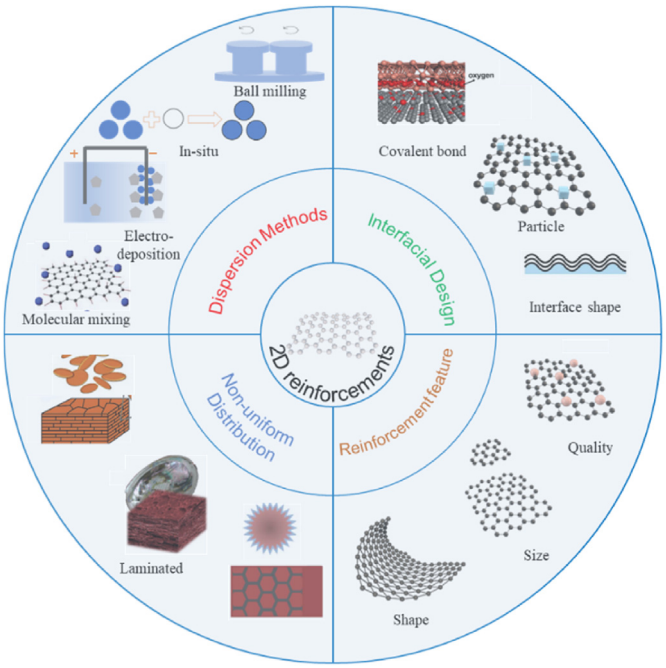

Fig. 12. Overview of the strategies for achieving exceptional properties in MMCs reinforced with 2D reinforcements. Taken from Refs. [81,93,94] with permissions.

ultimately resulting in disparities in the performance of 2D reinforcements. Thus, the investigation of performance variations in 2D reinforcements resulting from these disparities is of utmost significance. First, the researchers have studied the effects of different shapes of GN on the mechanics of MMCs through molecular dynamics (MD) simulations. By investigating boundary conditions of GN, Shuang et al. [82] deduced that the planar edges of GN played a crucial role in determining the mechanical properties of MMCs. Vardanyan et al. [83] concluded, by simulating the molecular dynamics of sheet and pleated GN in nickel-based composites, that sheet GN exerts an influence on the plastic deformation and mechanical properties of MMCs, while pleated GN exhibits a higher capacity for dislocation absorption (Fig. 13a). Therefore, it is imperative to consider the properties of different shapes of 2D reinforcements. In addition, the plane size of the 2D reinforcements can influence their strengthening effect. During the deformation process, the external mechanical load is transferred to the GN layer through the interface between GN and matrix following the shear lag model. Hence, the plane geometry of 2D reinforcements can impact their ability to transfer loads effectively. Moreover, in terms of length direction, similar to 0D and 1D reinforcements, 2D reinforcements exhibit extensive interactions with dislocations leading to the back stress strengthening, dislocation interlock, and dislocation annihilation. Zhao et al. [84] conducted compression of microcolumns of aluminum matrix composites with different plane sizes of GN and concluded that Taylor strengthening mechanism and back stress strengthening mechanism were the main strengthening mechanisms for improving the strength, compared with load transfer strengthening (Fig. 13c). Furthermore, the quality of 2D reinforcements can affect its enhancement effect because of their intrinsic properties. Li et al. [21] conducted microcolumn compression experiments on copper matrix composites reinforced by GN with different quality levels and concluded that interfacial shear strength and shear adjustment ability were related to GN quality (Fig. 13b). The low-quality 2D reinforcements in MMCs exhibit improved interfacial bonding with matrix due to its rough and defective surface, while high-quality 2D reinforcements effectively mitigate the degradation of functional properties.

4.2. Interface of 2D reinforcements

Given the extensive specific surface area of 2D reinforcements, it is no exaggeration to say that the interface bonding strength of reinforcements/metal matrix determines the performance of MMCs. The method proposed by Hwang et al. [74] for enhancing the interface strength of GN through functional group modifications demonstrated promising performance by transforming weak interfacial bonding into strong chemical bonding between GN and metal matrix (Fig. 14a). However, its implementation process is rather intricate and not conducive to large-scale promotion. Moreover, it is not possible to quantify the contribution of the improved interface strength to the material properties. On this basis, Androulidakis et al. [85] experimentally evidenced that corrugations in GN improve the load-bearing capability compared with flat GN. In addition, the research by Zhao et al. [86] investigated the GN/Cu nanocomposites by MD simulations and inferred that mechanical pre-strain can help generate wrinkles and increase roughness in GN. Thus, the interlocking effect between GN and Cu matrix can be remarkably improved (Fig. 14b). The combined use of wrinkles and functional groups in GN, may be a good choice, can improve the interfacial mechanical properties of GN/Cu nanocomposites dramatically. The interface reaction is additionally a viable approach to enhance the strength of the interface. The research findings of Jiang et al. [87] demonstrated that the interfacial reaction between GN and the matrix facilitates the formation of a well-oriented GN-Al_4C_3-Al interface, thereby significantly enhancing the interfacial bonding between GN and the matrix. Chu et al. [88] also revealed that through the reaction between GN and matrix, a well-bonded RGO-Cr_7C_3-CuCr interface could be realized, which not only improved the load transfer efficiency of GN but also enhanced its dislocation strengthening capability (Fig. 14c).

Further study of 2D reinforcements/metal interface shows that 2D reinforcements/metal interface exhibits distinct toughening mechanisms and deformation behavior because of large specific surface area, which differs from the blocking effect caused by 0D and 1D reinforcements with the relative dislocation movement. It is well known that dislocations cannot bypass or cut through 2D reinforcements because of the large size of its basal plane. Instead, they accumulate at 2D reinforcements/metal interface, causing stress concentration. The MD simulations conducted by Long et al. [89] demonstrated that GN could function as a dislocation source and provided nucleation sites when the critical resolved shear stress exceeded the energy required for dislocation nucleation. Especially in high strain rate deformation, the accumulation of large amounts of instantaneous strain around GN induced the occurrence of stacking faults and deforming twins [90]. In addition, the role of 2D reinforcements in the deformation process in the $Ti_3Al(Cu)C_2$-Cu system was thoroughly investigated by Zhang et al. [91] through a combination of *in situ* characterization and simulation. The findings demonstrate that 2D reinforcements serve as both barriers and dislocation sources.

4.3. Non-uniform distribution of 2D reinforcements

Thanks to the intricate microstructure, biological structural materials can achieve orders of magnitude increase in strength and toughness over their individual constituents. Many researchers have extensively studied the integration of biomimetic structures into metal-based materials to better balance mechanical and functional properties [92]. Xiong et al. [93] conducted a structural modelling of fir wood and fabricated layered GN reinforced copper matrix (Fig. 15a). The laminated GN with a significantly large specific surface area facilitated stress transfer, thereby enhancing the strengthening efficiency. Simultaneously, the "brick--and-mortar" structure greatly improves the elongation capability during crack propagation in the composite material, thereby achieving strong plastic synergy (Fig. 15b) [81]. Building upon this, Ni_3C is formed through carbon atom diffusion within the nickel matrix, resulting in a more continuous layered GN/nickel matrix composite [94]. Ni_3C not only acts as a load-bearing agent but also impedes crack propagation as

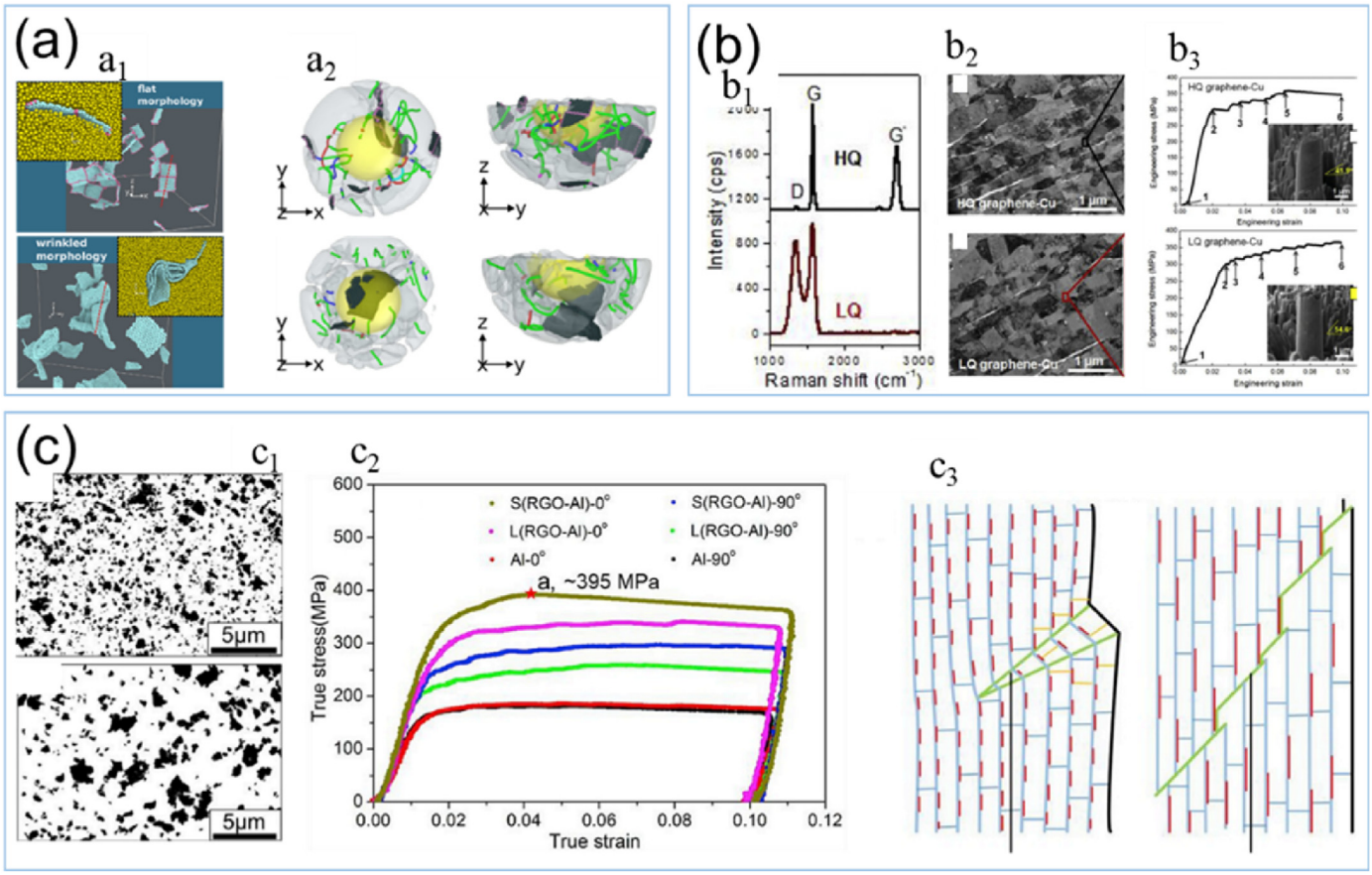

Fig. 13. Properties and mechanism of MMCs reinforced with 2D reinforcements based on the shape, quality, and size. (a) Reinforcements shape. $a_{1\text{-}2}$: flat and wrinkled morphology; a_3: top and side view onto the *x-y* plan of the plastic zone in the composite with flat morphology and wrinkled morphology [83]. (b) Reinforcements quality. b_1: Raman spectrums of HQ- and LQ-GN; b_2: TEM images of the as-fabricated HQ- and LQ-GN reinforced Cu composites; b_3: the representative engineering stress-strain curves of HQ (0.6 vol%) and LQ (1.8 vol%) GN-Cu composite micro-pillars [21]. (c) Reinforcements size. c_1: SEM images of GN; c_2: stress-strain of GN/Al; c_3: schematic illustration of the fracture mechanism [84]. Taken from Refs. [21,83,84] with permissions.

an obstacle. Additionally, fine crystals and interstitial atoms inhibit dislocation expansion and facilitate strength-plasticity synergy. Furthermore, applications of lamination demonstrate its effectiveness in 3D printing where layered GN/iron matrix composites are prepared using the powder bed melting technique. The interaction between GN nanoplatelets and the molten pool during the selective laser melting process leads to redistribution and relatively high-density non-uniform distribution of GN nanoplatelets within the molten pool. The high-density non-uniform distribution contributes to grain refinement and load transfer, effectively enhancing material strength while preventing hot cracks formation during printing. In addition, a systematic study on the rate-dependent deformation behavior of GN/Cu sub-micro-laminated composites was performed by splitting Hopkinson pressure bar tests for high strain rate loading and laser-induced projectile impact tests for extreme strain rate loading, and the study suggests that the deformation mechanism of MMCs changes to GN-assisted twins induced by high strain conditions [95].

4.4. Summary of the attainable mechanical properties of MMCs reinforced with 2D reinforcements

The correlation between the content of 2D reinforcements and the normalized strength and elongation, as obtained from the literature, is illustrated in Fig. 16. It can be seen that, with the increase of the content of 2D reinforcements, the strength of MMCs increases at the expense of the elongation. The heterogeneous distribution of 2D reinforcements, as indicated by the current data, partially enhances this phenomenon. Nevertheless, there is still significant untapped potential for further development in 2D reinforcements concerning strength improvement.

5. Metal matrix composites reinforced with 3D reinforcements

At present, researchers around the world have made significant progress in the study of MMCs reinforced with 0D, 1D and 2D reinforcements, including strength, modulus, plasticity, toughness, etc., and even made breakthroughs in the strength and plasticity that have plagued researchers for a long time. However, 0D, 1D and 2D reinforcements, limited in size, exert influence on the plastic deformation behavior of the matrix mainly by modulating dislocation behavior [49,91]. In contrast, 3D reinforcements magnify these micro-region responses, thereby impacting grain structure, grain boundaries, and even macroscopic deformation texture due to the continuity of 3D reinforcements in the whole matrix space [22,96]. Over the past few decades, nanostructured metals (with grain size below 100 nm) exhibit ultrahigh strength and hardness, making them very attractive for developing novel lightweight and energy-efficient structural components [97,98]. However, when the grain size in nanostructured metals is reduced to the nanometer scale, it leads to the attainment of ultra-high strength while rendering grain boundary highly unstable. Consequently, certain nanostructured materials undergo coarsening even at room temperature, thereby significantly impacting their performance in engineering applications [99]. Therefore, it is important to improve the grain boundary stability of nanostructured materials. Thermodynamically, lowering grain boundary energy can reduce the driving force for

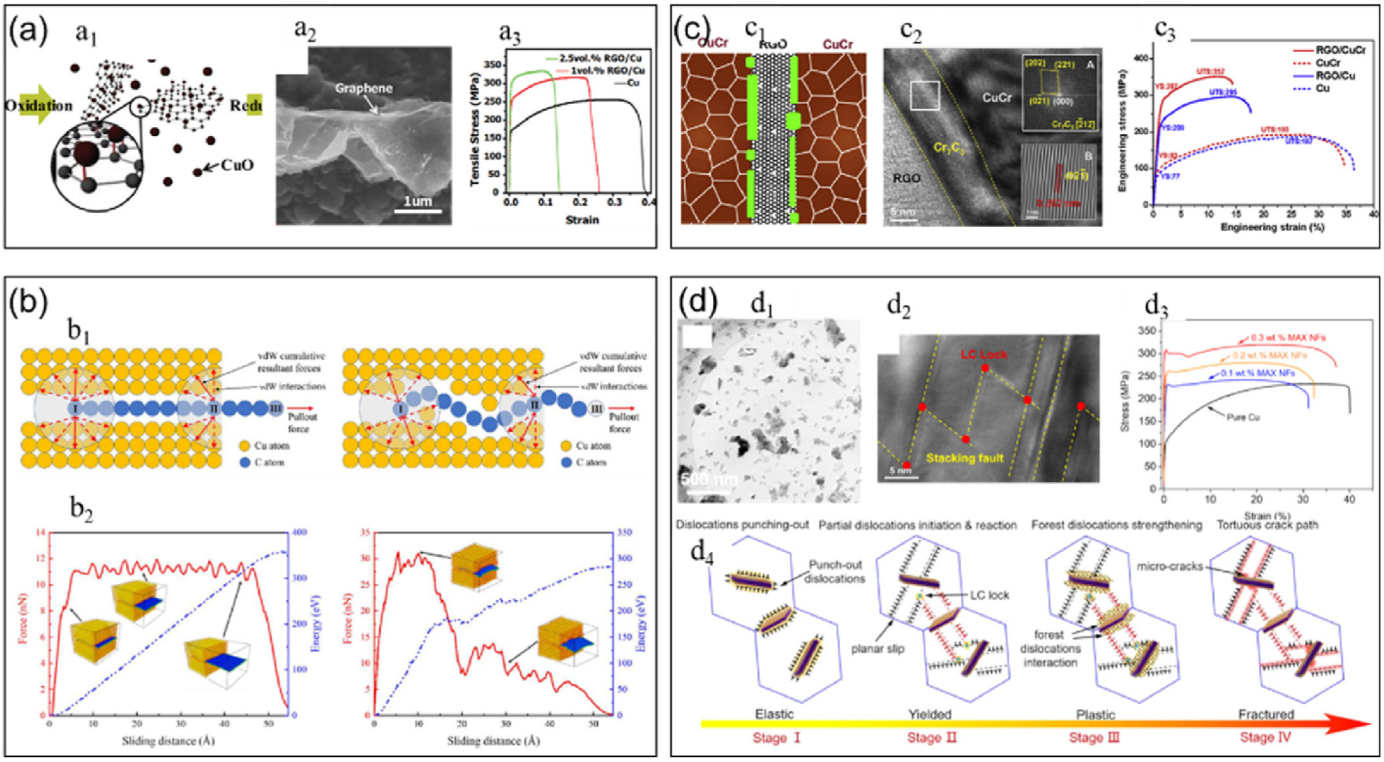

Fig. 14. Microstructure, properties and mechanism of MMCs reinforced with 2D reinforcements based on interfacial design. (a) Covalent bond. a_1: schematic illustration of CuO-GN; a_2: SEM image of GN; a_3: stress-strain curves of RGO/Cu [74]. (b) Interface shape. b_1: schematic of the cumulative vdW forces of flat and wrinkled GN during the pull-out process; b_2: the pull-out force and potential energy change [86]. (c) Particles. c_1: schematic of RGO-CuCr interface; c_2: HRTEM images of RGO-CuCr interface; c_3: stress-strain curves of RGO/Cu and RGO/CuCr. (d) Deformation control [88]. d_1: TEM image of the ultrasonication-exfoliated nanoflakes from $Ti_3Al(Cu)C_2$; d_2: HRTEM image showing the hierarchical SFs network and Lomer-Cottrel locks; d_3: stress-strain curves of MAX NFs/Cu; d_4: schematic illustrations of microstructural evolution during plastic deformation [91]. Taken from Refs. [74,86,88,91] with permissions.

grain coarsening. This is often achieved by solute segregation, such as in Ni-W, Co-P, and Ni-Fe alloys [100]. In addition, using low angle boundary or twin boundary dispersion in pure Cu or Ni can stabilize nanostructures as well. Kinetically, the driving force for grain coarsening could be counteracted by precipitate particles pinning the grain boundaries. This is normally achieved by mechanical alloying, such as in Cu-WC and Cu-Ta alloys [101]. The stability of the nanostructure can be further enhanced when thermodynamic and kinetic strategies are favorably combined together by 3D reinforcements. Furthermore, the incorporation of 3D reinforcements into MMCs, unlike 0D, 1D and 2D reinforcements, has a change to break through the compromise of functional properties such as electrical and thermal conductivity due to the continuous network topology. These composites exhibit unique and extraordinary performance matching, such as strength and damping [102], thermal conductivity and mechanical properties [103] and strength and conductivity [104]. Therefore, the utilization of MMCs reinforced with 3D reinforcements is anticipated to overcome the limitations of conventional MMCs and accomplish seamless integration of structure and function (see Table 1).

In this section, we first define and classify 3D reinforcements, and the preparation method and distinctive properties of MMCs reinforced with 3D reinforcements are concisely presented.

5.1. Definition of 3D reinforcements

We define the reinforcements with completely continuous distribution between grain boundaries as 3D reinforcements, as shown in Fig. 17. Currently, there are two primary strategies employed for the formation of the 3D reinforcements: the continuous composition of precipitates at the grain boundary and comprise of assembly of precursor powders via powder metallurgy. The continuity of reinforcements serves as a crucial foundation for our division. Moreover, 3D reinforcements exhibit distinct performance control mechanisms compared with 0D, 1D and 2D reinforcements. Next, we elaborate on the preparation method, material properties and specific regulatory mechanisms such as strengthening and toughening mechanisms, dislocation behavior, stress regulation and fracture behavior.

5.2. Classification of 3D reinforcements

In recent years, the 3D reinforcements, through architecture design of the spatial structure of reinforcements, have shown incredible improvement in mechanical performance and have achieved extraordinary functional properties such as electrical and thermal conductivity, making them promising reinforcements for MMCs with multifunctional properties. As shown in Fig. 17, based on the fabrication strategy of 3D reinforcements, the continuous 3D network reinforcement could be classified into two main categories, including continuous precipitates and precursor powders. Subsequently, we give a detailed introduction and summary of the two preparation processes for the formation of 3D reinforcements. Next, our focus is on understanding the influence of 3D reinforcements on the comprehensive properties of MMCs.

5.2.1. Continuous precipitates

Grain boundary engineering is a versatile tool for strengthening materials by tuning the composition and bonding structure at the interface of neighboring crystallites, and this method holds special significance for materials composed of small nanograins where the ultimate strength is dominated by grain boundary instead of dislocation motion [105,106]. The formation of continuous precipitates takes advantage of the segregation of elements at grain boundaries. These 3D reinforcements can not only improve the stability but also enhance the plasticity of MMCs. The

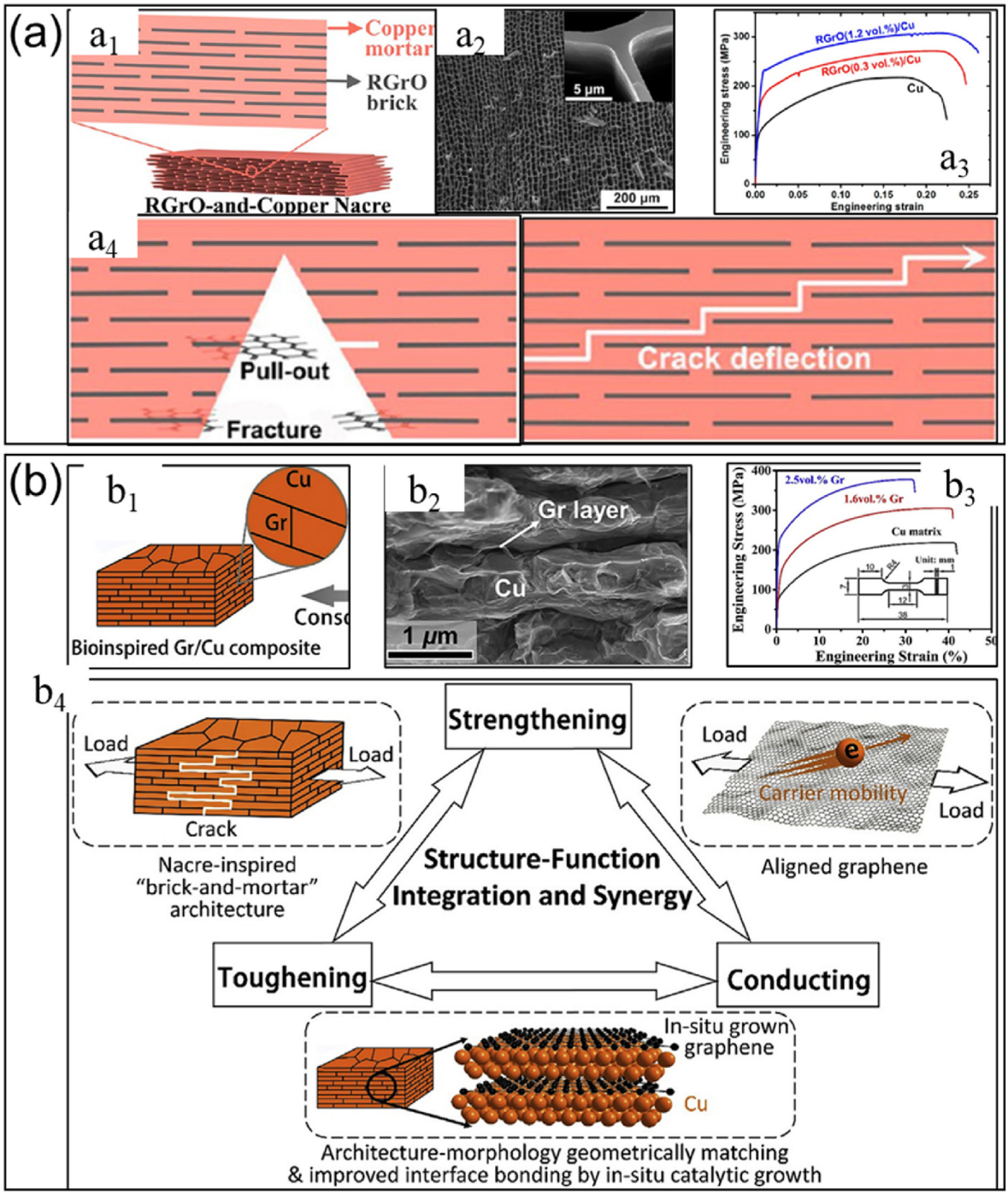

Fig. 15. Microstructure, properties and mechanism of MMCs reinforced with laminated architrcture 2D reinforcements. (a) a_1: RGrO-and-copper nacre consisting of RGrO "brick" and copper "mortar"; a_2: monolithic fir-templated porous Cu; a_3: tensile stress-strain curves of the RGrO-and-Cu nacres; a_4: schematic representation of failure modes of the RGrO [93]. (b) b_1: nacre-inspired composite; b_2: SEM image of the local stacking of flakes; b_3: engineering stress-strain curves for Gr/Cu composites and the unreinforced Cu matrix; b_4: schematic illustration showing structure-function integration and synergy [81]. Taken from Refs. [81,93] with permissions.

crack-fee Haynes 230 alloy was prepared by taking advantage of the segregation of Zr atoms and abundant cell boundaries to relieve the stress/strain concentration and coordinate grain deformation through the introduction of stable liquid backfilling and a networked intermetallic $Ni_{11}Zr_9$ phase by Zhao et al. [107]. The continuous 3D network of the intermetallic $Ni_{11}Zr_9$ phase is observed to act as a "skeleton", which significantly improves the yield strength of the as-printed sample by more than 50 % (Fig. 18a). The authors deem the segregation engineering and abundant cell boundaries to introduce liquid backfilling as well as a network of segregation phases to alleviate thermal stress, consequently eliminating hot cracking. Moreover, this continuous $Ni_{11}Zr_9$ 3D network layer can act as a *skeleton* to significantly improve the yield strength of the composite. Lu et al. [108] designed and constructed a "bamboo-like" nanocolumnar copper structure reinforced by an amorphous boron framework that served as a strong and robust thick grain boundary 3D network (Fig. 18b). The significant strengthening effect is realized by the delicate design of a nanocolumnar copper film that comprises columnar nanograins embedded in a bamboo-like boron

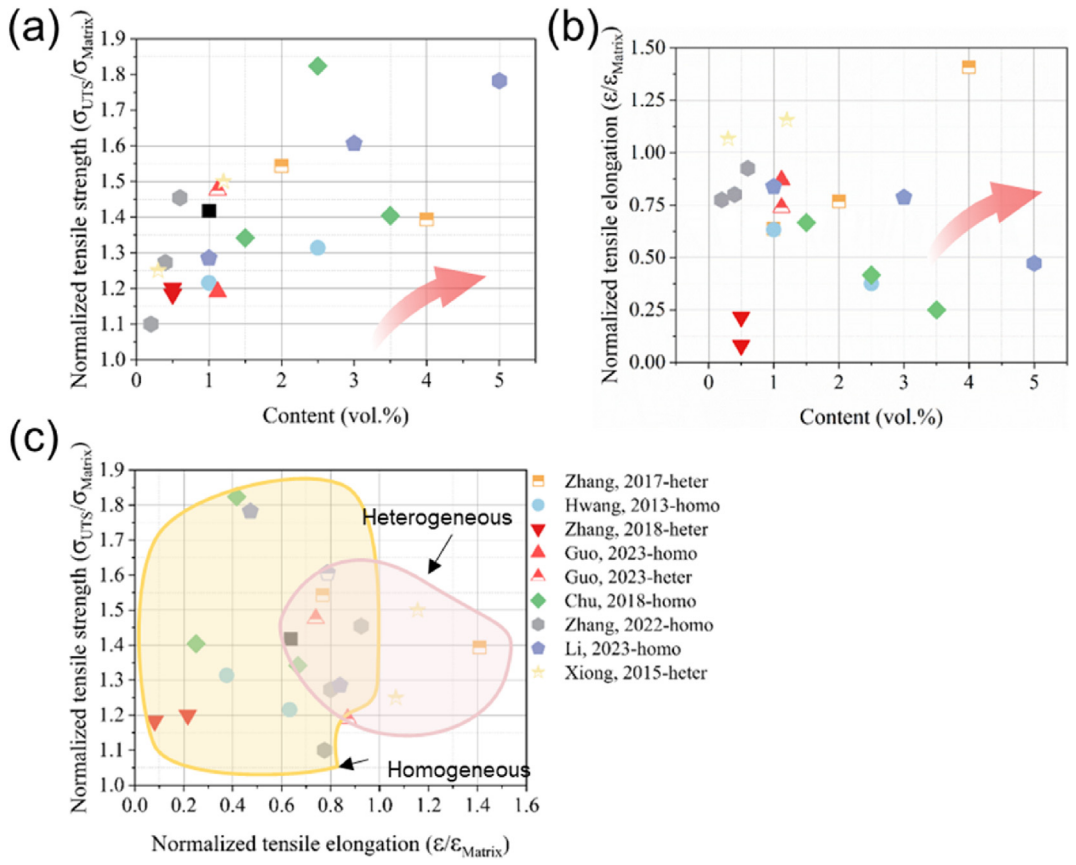

Fig. 16. Maps of (a) normalized tensile strength versus the content of 2D reinforcements, (b) normalized tensile elongation versus the content of 2D reinforcements and (c) normalized tensile strength versus normalized tensile elongation of MMCs reinforced with 2D reinforcements [69,71,74,78,79,88,91,93].

Table 1
Properties of MMCs reinforced with 3D reinforcements.

Matrix	Reinforcements	YS (MPa)	UTS (MPa)	Fracture strain (%)	Property	Ref.
Ni	$Ni_{11}Zr_9$ network	621	1023	35	alleviate thermal stress	[107]
$(Mn,Fe)_2(P,Si)$	Cu network		390		high thermal conductivity and strength	[103]
Cu	grain network	396	502	~13	high strength and large ductility	[115]
Cu	bamboo-like dual-phase network	1360	2580	~50	ultrahigh strength and ductility	[108]
FeCoNiAlTi	dislocation-precipitate network	1420	1760	~16	good structural stability	[116]
Ti	Ti6Al4V network	535	~590	20	high strength and fracture toughness	[117]
Ti6Al4V5Cu	dual-phase honeycomb shell	1400	1520	12	high strength, ductility and stability	[96]
TiZr	crystalline-amorphous network	1800	2300	~7	ultrahigh strength and ductility	[118]
Cu	GN network	292	319	24.4	high strength, ductility, thermal and electrical conductivity	[22]
Mg	NiTi network	320		45	improved strength, remarkable damage tolerance, damping capacities and energy absorption efficiency	[102]

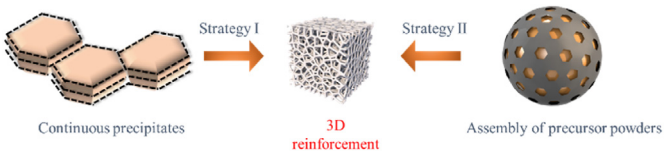

Fig. 17. Methods to prepare MMCs reinforced with 3D reinforcement.

framework obtained by magnetron sputtering co-deposition. The nano-indentation hardness reaches an extremely high level of 10.8 GPa, surpassing most of the currently reported Cu alloys. The authors believe that the deformation process is closely related to GB complexion, which limits dislocation propagation by the ledges and solute atoms at the grain-complexion interface, thus resulting in strong dislocation pinning and increasing the flow stress required for dislocation movement. Thick grain boundaries can also effectively prevent dislocation propagation by acting as a dislocation sink. In addition, bamboo-like 3D structures can achieve better resistance to shear processes through improved bending response, thus leading to superb mechanical performance. Wang et al. [96] presented a pathway to achieve ultrastable nanosized grains by constructing a "dual-phase honeycomb shell" nanostructure through a low-cost "eutectoid element alloying-auenching-hot deformation" strategy in a $Ti_6Al_4V_5Cu$ model alloy (Fig. 18c). As a result, the key challenge

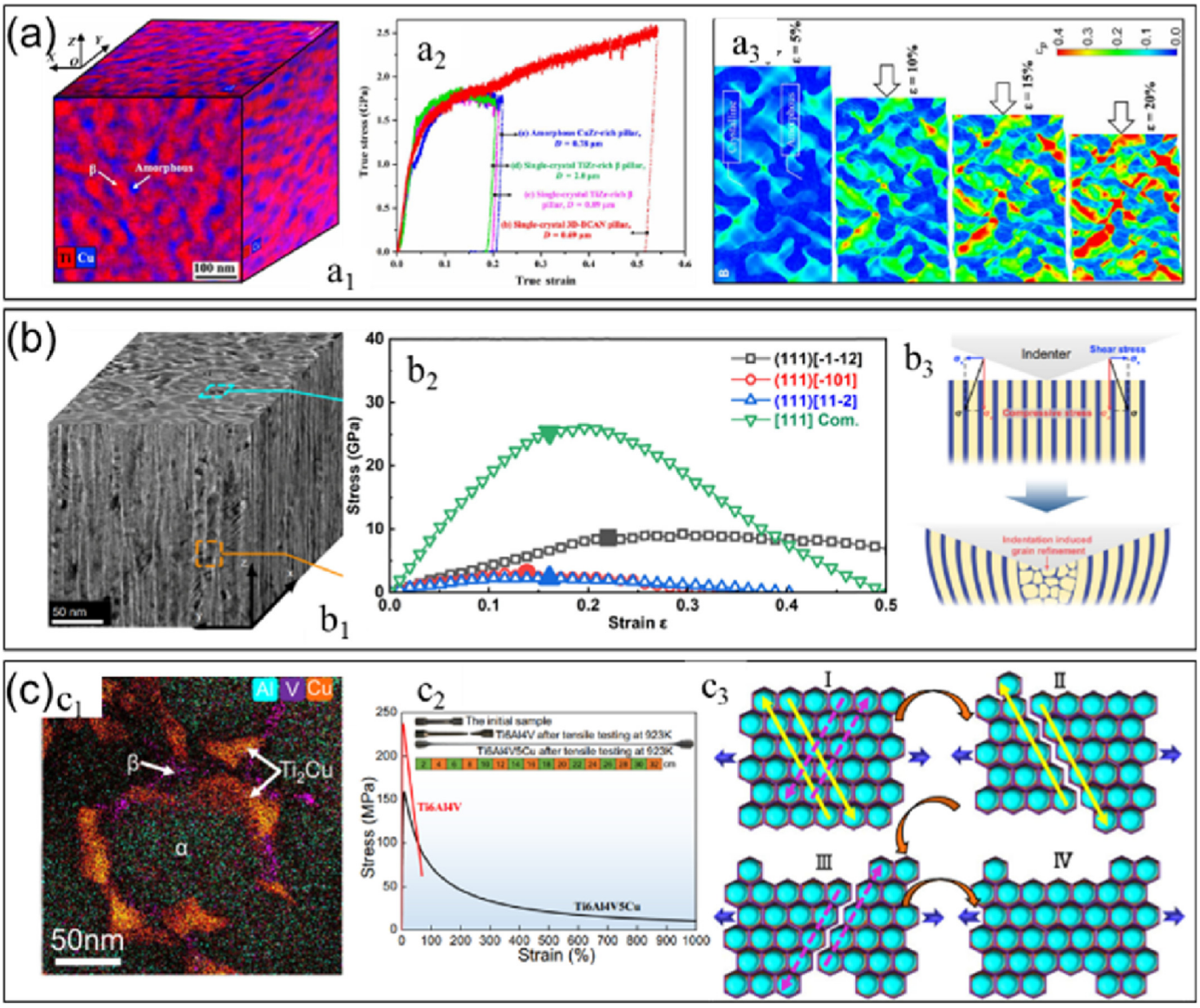

Fig. 18. Microstructure, properties and mechanism of MMCs reinforced with 3D reinforcements via continuous precipitates. (a) Three-dimensional structure of the bicontinuous TiZr-based alloy. a_1: TEM-energy dispersive spectroscopy mapping of Ti and Cu elements; a_2: true stress-strain curves of the bicontinuous TiZr-based alloy in compression tests; a_3: snapshots highlight the evolution of the equivalent plastic strain during compression [107]. (b) Three-dimensional bamboo-like dual-phase Cu-B nanocomposite. b_1: 3D TEM image of the bamboo-like dual-phase structure; b_2: calculated stress responses of Cu under the shear strains in the (111) plane; b_3: schematic illustration of the mechanical response of dual-phase Cu-B [108]. (c) Three-dimensional dual-phase honeycomb shell Ti6Al4V5Cu alloy. c_1: Ti and Cu distribution; c_2: stress versus strain curves at 923 K; c_3: schematic flowchart of the superplastic mechanism [96]. Taken from Refs. [96,107,108] with permissions.

to retain nanosized grains in metal bulk forming processes has been effectively overcome. The authors consider that the conjugated β and Ti_2Cu not only inhibit grain coarsening during the high-temperature fabrication process but also significantly enhance the stability of the nanostructure against post-fabrication annealing. More important, regions with larger strains always corresponded to the place where significant phase interface slip occurred, therefore, the superplastic deformation should be governed by phase boundary sliding. Then, MMCs reinforced with the 3D GN network were prepared by the molding process.

5.2.2. *Assembly of precursor powders*

The precursor powders are prepared by coating a solid or liquid source on the metal powders and ex-situ or *in situ* synthesizing reinforcements at the grain boundary. By modifying the surface of TC4 particles with polyvinyl alcohol, Zhang et al. [109] rendered spontaneous adsorption of GN onto the surface of TC4 particles and prepared network GN/TC4 composite, which exhibited higher compressive strength and ductility owing to the capability of the network to alleviate stress concentration and enhance grain refinement. Zhang et al. [22] firstly reported a powder-metallurgy-based strategy to construct a 3D continuous GN network in the copper matrix through thermal-stress-induced welding between GN-like nanosheets grown on the surface of copper powders (Fig. 19a). The interpenetrating structural feature of the as-obtained composites not only promotes the interfacial shear stress to a high level and thus results in significantly enhanced load transfer strengthening and crack-bridging toughening simultaneously but also constructs additional 3D hyper channels for electrical and thermal conductivity. It provides theoretical and experimental guidance for the preparation of structure-function integrated MMCs. Additionally, subsequent research conducted by the research group further demonstrated the capability of a 3D continuous GN network to effectively coordinate deformation and strain delocalization during dynamic deformation, while also effectively limiting grain growth at elevated temperatures [110,111] (Fig. 19b–c). In

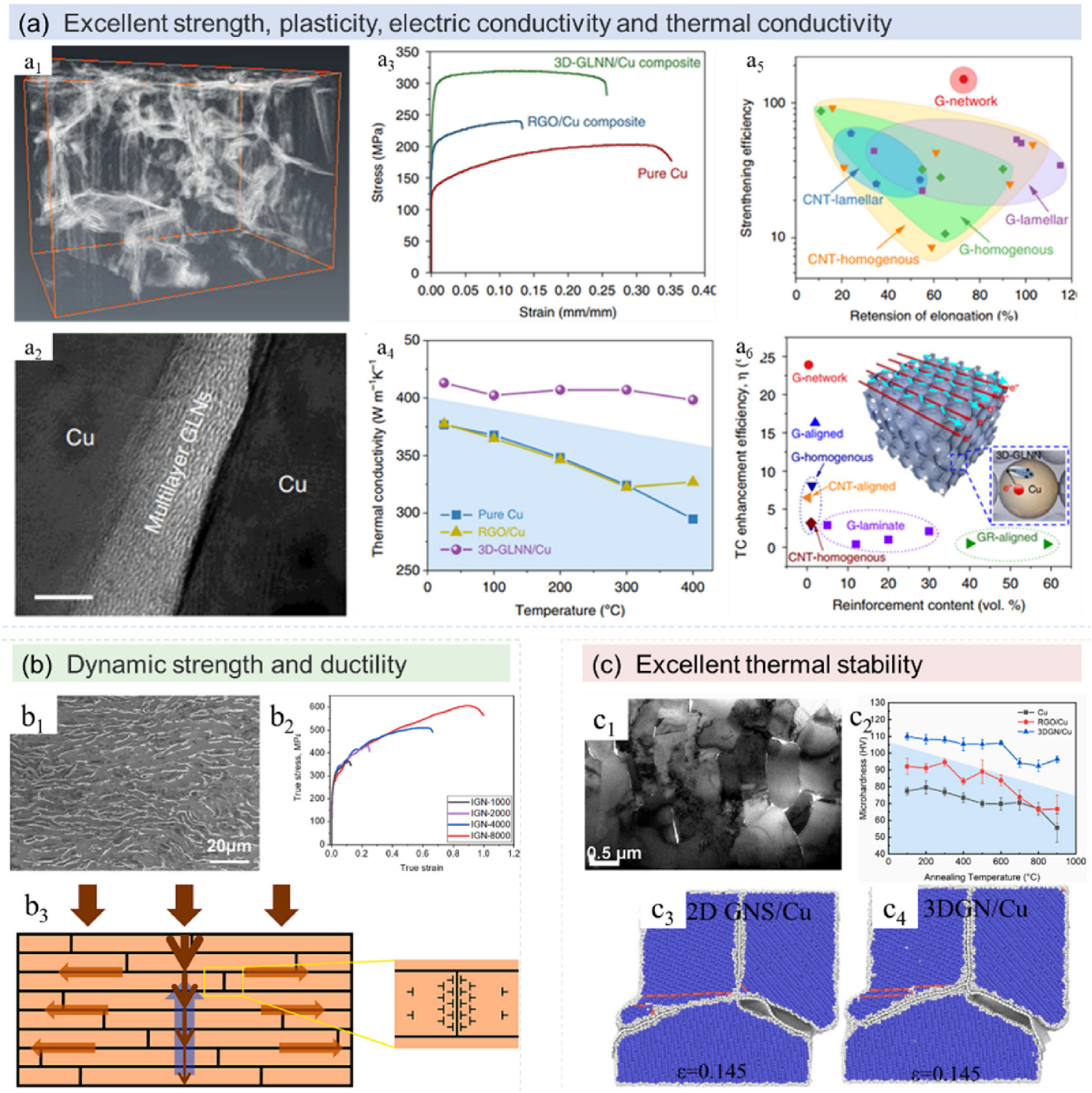

Fig. 19. Microstructure, properties and mechanism of MMCs reinforced with 3D reinforcements via M@C powders. (a) Excellent strength, plasticity, electric conductivity and thermal conductivity in 3D GN/Cu. a_1: snapshot of FIB-3D reconstruction results of 3D GN/Cu; a_2: TEM image of 3D GN/Cu; a_3: tensile stress-strain curves; a_4: the in-plane thermal conductivities; a_5: the retention of fractural elongation versus strengthening efficiency; a_6: the TC enhancement efficiency versus GN content plot [22]. (b) Excellent dynamic strength and ductility. b_1: SEM image of the GN network; b_2: dynamic compressive stress-strain curves; b_3: illustration of the interaction between shock waves and GN interfaces [110]. (c) Excellent thermal stability. c_1: TEM images of 3D GN/Cu annealed at 800 °C for 1 h in air; c_2: room temperature hardness after annealing at different temperatures for 1 h in air; c_3, c_4: atom snapshot of grain boundary migration under different strains [111]. Taken from Refs. [22,110,111] with permissions.

addition, MD results proposed by Yang et al. [112,113] showed that the interlocking structure improves the deformation compatibility between GN and matrix, as well as increases the load-sharing of GN. And, the mechanical interlocking can be further enhanced by the dislocation-GN interactions as GN is straightened. The straightening of GN also enables it to release its stress concentrations through overall deformation, which helps the GN perform better in dislocation blocking than GN sheets. Besides, curved portions of GN contribute more to dislocation-GN interactions while the straight portions do better in load-sharing. On this basis, the novel 3D GN reinforced Cu composites were successfully fabricated by vacuum hot-press sintering Cu powders and non-toxic, cheap liquid paraffin [114]. As a result, the cold-drawn Cu/GN composite wire exhibits high electrical conductivity of 94.85 % IACS and high tensile strength of 516 MPa, together with good softening resistance. The authors believe that the uniformly distributed 3D GN plays a vital role, which acts as an electron transport channel and strengthens the

matrix by grain refinement, dislocation strengthening and load transfer mechanisms.

5.3. Summary of the attainable mechanical properties of MMCs reinforced with 3D reinforcements

The normalized strength and elongation data of MMCs reinforced with 0D, 1D, 2D and 3D reinforcements, obtained from the literature, are depicted in Fig. 20. It can be seen that 0D reinforcements have a high reinforcement effect, but it is also accompanied by the problem of reduced elongation. Correspondingly, the incorporation of 3D reinforcements has a significant impact on enhancing elongation. However, the improvement in strength falls short of expectations, possibly due to incomplete development of 3D reinforcements. In addition, the enhancement effect of 1D and 2D reinforcements for strength and elongation is between 0D and 3D reinforcements.

6. Strengthening mechanisms and plastic deformation mechanisms

6.1. Strengthening mechanisms

The strengthening mechanisms of MMCs reinforced with different dimensional reinforcements should not only consider the intrinsic strength of reinforcements and their interfaces but also take into account the interaction between reinforcements and dislocations, as well as the mismatch between reinforcements and matrix caused by different intrinsic properties during processing or deformation [3,119]. Additionally, it is crucial to consider the non-uniform distribution of reinforcements because of their unique strengthening mechanisms such as high work hardening rate [120]. Therefore, the strengthening mechanisms primarily involve Hall-Petch strengthening, Orowan strengthening, dislocation strengthening, HDI strengthening and load transfer strengthening.

6.1.1. Hall-Petch strengthening mechanism

The Hall-Petch strengthening is attributed to grain refinement resulting from the introduction of small-size reinforcements, of course, the size of the reinforcements is above the critical size, which can be expressed as [121].

$$\sigma_{P-L} = \frac{k_0}{\sqrt{D}} \tag{1}$$

where k_0 is a material constant and D is mean grain size. Generally speaking, the smaller the grain size of MMCs, the higher the strength of Hall-Petch strengthening. The variation in grain refinement mechanism among reinforcements of different dimensions is worth noting, as it can be attributed to differences in dynamics and thermodynamics. On the one hand, uniformly dispersed heterogeneous or semi-coherent/coherent particles thermodynamically contribute to the refinement of grains among MMCs reinforced with 0D or low aspect ratio 1D reinforcements [30,56]. On the other hand, from the perspective of dynamics, the high density 1D reinforcements distributed between grains, the 1D and 2D reinforcements with high aspect ratio or specific surface area, and the complete continuity 3D reinforcements can effectively limit the grain growth [96,122].

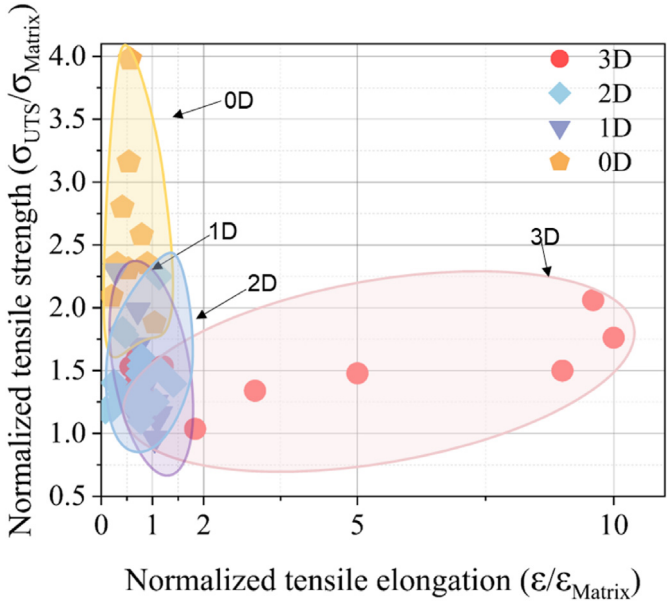

Fig. 20. Maps of normalized tensile strength versus normalized tensile elongation of MMCs reinforced with 0D, 1D, 2D and 3D reinforcements [10,20,22,34,38–40,48,62,63,69,71,79,88,91,93,96,102,107,115–117].

6.1.2. Orowan strengthening mechanism

The phenomenon of Orowan strengthening arises from the interaction between reinforcements and dislocations. When dislocations are unable to cut but bypass the low-size reinforcements, they form an Orowan ring adjacent to the reinforcements region, thereby resulting in Orowan strengthening. The yield strength caused by Orowan strengthening can be expressed [123].

$$\sigma_{Or} = O\frac{0.4Gb}{\pi(1-\nu)^{\frac{1}{2}}}\frac{\ln\left(\sqrt{\frac{2}{3}}d/b\right)}{\lambda} \tag{2}$$

where O is mean orientation factor, G is shear modulus, b is Burgers vector, ν is Poisson's ratio, d is average diameter of reinforcements, and $\lambda = \sqrt{\frac{2}{3}}d\left(\sqrt{\frac{\pi}{4f}}-1\right)$ with f being the volume fraction of reinforcements.

In addition, some studies suggest that 1D reinforcements with low aspect ratios, usually less than 10, also exhibit significant Orowan strengthening, which can be quantified as [124].

$$\sigma_{Or} = \frac{GbM}{2.36\pi(\lambda-d)}\ln\left(\frac{d}{2b}\right) \tag{3}$$

where λ is interparticle spacing; M is Taylor's factor. The size and content of reinforcements are generally considered to be the primary factors in the Orowan strengthening mechanism. However, the Orowan strengthening effect of MMCs with high content reinforcements is significantly reduced from its theoretical value due to the limited dislocation slip. Furthermore, the Orowan strengthening mechanism is unlikely to be attributed to 2D and 3D reinforcements with large specific surface areas, as dislocations cannot bypass them.

6.1.3. HDI strengthening mechanism

During the plastic deformation, stress is preferentially concentrated around reinforcements, due to the substantial disparity in strength, hardness and modulus between reinforcements and matrix [125]. As the deformation increases, a strain gradient develops as a result of varying deformation abilities between reinforcements and matrix. To counteract this strain gradient, it is necessary to form the pile-up structure of GNDs near the interface. This process leads to the generation of back stress in the matrix and forward stress around reinforcements, ultimately resulting in HDI strengthening. Take 1D reinforcements as an example, the σ_{HDI} can be expressed as [20]

$$\sigma_{HDI} = M\frac{\mu b}{d}\left(\left\{n^0\left[\left(1-\left(1-\frac{S}{1-s^2}\right)\right)\frac{n^0}{n_0^*}\right]\right\}\right) + (\gamma D\mu V_0\varepsilon_p) \tag{4}$$

where n_0^* is maximum number of loops around 1D reinforcements; d is mean diameter of 1D reinforcements; γ is local plastic strain; ε_p is unrelaxed plastic strain. In other words, the numerous heterogeneous interfaces caused by the introduction of high-density reinforcements into the matrix contribute to the accumulation of the number of GDNs, which improves the effect of HDI strengthening. In addition, the MMCs reinforced with non-uniformly distributed reinforcements or 3D continuous reinforcements exhibit a more pronounced HDI strengthening effect compared to the MMCs reinforced with uniformly distributed reinforcements, attributed to the superposition of plastic deformation zones or interfacial action zones [50,126].

6.1.4. Dislocation strengthening mechanism

The yield strength caused by dislocations reads

$$\sigma_{Dis} = \alpha G\sqrt{\rho_{Dis}} \tag{5}$$

where α is constant; ρ_{Dis} is density of dislocation. Moreover, ρ_{Dis} contains the coefficient of thermal expansion (CTE) mismatch (ρ_{CTE}) and elastic modulus mismatch (ρ_M) and can be expressed as [127]

$$\rho_{Dis} = \rho_{CTE} + \rho_M = \frac{12f(\Delta c\Delta T)}{(1-f)bd} + \frac{8f\varepsilon_1}{bd} \tag{6}$$

where ΔC is CTE mismatch between particles and matrix, ΔT is temperature change during processing, and ε_1 is yielding strain.

6.1.5. Load transfer strengthening mechanism

The load transfer strengthening is attributed to the transmission of load from the matrix to reinforcements through an interface, where the area and strength of the interface determine the extent of load transfer strengthening [128]. The 1D or 2D reinforcements with a high aspect ratio or specific surface area naturally exhibit enhanced load-bearing capabilities than 0D reinforcements because of the premature failure in MMCs with high-density particles, without considering the influence of interface bonding strength. Specifically, the load transfer strengthening effect depends on the interface bonding strength between reinforcements and matrix, which is closely associated with the aspect ratio or surface area of reinforcements [129]. Here we utilize MMCs reinforced with 2D reinforcements as an illustrative example, the σ_{L-T} can be expressed as [57]

$$\sigma_{L-T} = \frac{1}{2}\tau S v_f + \sigma_m(1-v_f), S < S_0 \tag{7}$$

$$\sigma_{L-T} = \left(1 - \frac{\sigma_m}{2\tau S}\right)\sigma_m v_f + \sigma_m(1-v_f), S > S_0 \tag{8}$$

where τ is interfacial shear strength; v_f is volume fraction of 2D reinforcements; S_0 is critical aspect ratio of 2D reinforcements, given by $S_0 = \sigma_f/\tau_m$; σ_f is tensile strength of 2D reinforcements; τ_m is yield shear strength of matrix; σ_m is tensile strength of matrix. In additional, the orientation of 1D reinforcements shows a great influence on the effect of load transfer strengthening and the model can be expressed as [128] when $S \le S_\theta$,

$$\sigma_{L-T} = \frac{1}{2}\sigma_0 V_0\left[S\cos^2\theta + \left(1+\frac{1}{S}\right)\left(1-\frac{4}{3\pi}\right)\sin^2\theta\right] \tag{9}$$

when $S \ge S_\theta$,

$$\sigma_{L-T} = \sigma_{1D}V_0\cos\theta\left(1-\frac{S_\theta}{2s}\right) + \frac{1}{2}\left[\left(3-\frac{4}{3\pi}\right)\sin^2\theta - 2 + \frac{1}{S}\left(S_\theta\cos^2\theta + \sin^2\theta - \frac{4\sin^2\theta}{3\pi}\right)\right] \tag{10}$$

where S_θ is off-axis critical aspect ratio; V_0 is volume fraction of 1D reinforcements; S is whisker-aspect ratio, and θ is certain off-axis angle; σ_{1D} is ultimate tensile strength of 1D reinforcements. Note that the deformation mechanism of MMCs reinforced with 1D reinforcements is changed from the pipe diffusion mechanism to the dislocation climb controlled by lattice diffusion at high temperature. Notably, previous studies suggested that the MMCs with 3D reinforcements have a rich number of interfaces and firm interface strength, resulting in obvious load transfer strengthening. However, the exact contributing factors are unclear.

6.2. Plastic deformation mechanisms

6.2.1. Zero-dimensional reinforcements

(1) *Work hardening.* For metal materials, the work hardening rate (θ) is an important indicator to measure the plasticity and toughness of the materials before the onset of plastic instability (necking), which can be governed by Hart's criterion as follows [130]:

$$\theta + m\sigma \le \sigma \tag{11}$$

where $\theta = \frac{d\varepsilon}{d\sigma}$, and m is constant generally less than 0.05 for metallic materials. Therefore, the high work hardening rate is crucial for enhancing the plastic deformation ability and toughness of MMCs. In the initial stage of plastic deformation, a high density of dislocations is observed due to the strong pinning of particles on the dislocation, as depicted in Fig. 3a. When a dislocation bypasses a particle, it forms an Orowan ring around the particle which subsequently interacts with other dislocations due to the back stress, leading to an additional increase in work hardening rate. As the applied load further increases, a higher density of dislocations are formed, resulting in stress concentration around the particles. To effectively manage these stress concentrations, dislocation nucleation can occur on other primary slip planes as well as on secondary slip planes, thereby facilitating interaction between multiple slip planes and enhancing the work hardening rate [28].

(2) *Fracture behavior.* It is well known that the toughness of a composite is related to the energy dissipation during plastic deformation, crack nucleation and crack propagation [131]. There are two types of toughening mechanisms in MMCs reinforced with 0D reinforcement: intrinsic and extrinsic toughening. In the process of deformation, cracks preferentially nucleate at the particle/metal interface, and as the size of particles decreases, a transition occurs from a particle/matrix interface-dominated failure initiation to a dislocation punched zone-matrix boundary-dominated failure initiation, in the case of a well-bonded particle/matrix interface. Therefore, cracks are more likely to nucleate at the NPR/NPF interface due to the small distance between particles, which reduces crack nucleation and improves toughness.

The cracks bridge and deflection are important extrinsic toughening mechanisms. Thus, the determination of whether the crack propagates across or circumvents the interface is crucial to the toughness of MMCs reinforced with 0D reinforcement. The characteristic dimension R_0 of the crack tip's "plastic zone" can be estimated by [132]

$$R_0 = \frac{0.26d^2E^2}{\pi V^{\frac{1}{3}}} \tag{12}$$

where d is size of particles; V is volume fraction of particles. R_0 is different between NPF and NPR zones due to the non-uniform distribution of particles, which leads to the cyclical change of R_0 of NPF and NPR zones. Thus, the toughness of MMCs reinforced with 0D reinforcements could be significantly increased via the extrinsic toughening mechanism.

6.2.2. One-dimensional reinforcements

(1) *Dislocation behavior*. Studying the interaction between interface and dislocations is crucial considering the large aspect ratio of 1D reinforcements. When dislocation encounters 1D reinforcements with a small aspect ratio, a strong interaction occurs, resulting in the formation of the Orowan ring near reinforcements, which effectively provides forest hardening and back stress hardening while activating cross slip of dislocation (Fig. 8). Conversely, dislocation is hindered from passing through 1D reinforcements with a large aspect ratio during dislocation motion, leading to the accumulation of dislocations near reinforcements. The deformation process is dominated by the competition between the multiplication and annihilation of dislocations near 1D reinforcements with a large aspect ratio. This leads to a high strain hardening rate and improved elongation. Sadeghi et al. [133] proposed a method to study dislocation behavior by evaluating the ratio of the grain interior/grain boundary affected zones (GI/GBAZ). The 1D reinforcements with a large aspect ratio are situated in the GBAZ, and during the deformation, the GBAZ thickness is mainly influenced by the number of mobile dislocations, leading to fluctuations in local plastic strain and arbitrariness in selecting slip systems. Moreover, the GBAZ thickness in grains significantly affects the driving force required for dynamic recrystallization (DR) and DRX, as well as total dislocation density and mean free path for dislocation. Thus, modifying the GBAZ thickness could effectively adjust dislocation behavior.

Besides the intrinsic interfacial structure, the non-uniform distribution of 1D reinforcements also plays an important role in influencing the dislocation behavior, as shown in Fig. 9. It is demonstrated that the initial stage of plastic deformation is characterized by the preferential accumulation of dislocations near 1D reinforcements, leading to localized stress concentration within the hard phase. This accumulation results in the development of a strain gradient and subsequently facilitates the formation of GNDs. Concurrently, adjustments take place within the soft phase in response to this strain gradient, with the increase in the stress variable, dislocation density within the soft phase also rises. This increase ultimately results in dislocations accumulating at grain boundaries until crack initiation occurs.

Furthermore, the introduction of 1D reinforcements may also facilitate to production of stacking faults. Guo et al. [134] found the stacking faults in CNTs/Al composites, which were validated to be caused by the high strain rate and reduction in the stacking fault energy facilitated by CNTs. The formation of stacking faults thus in turn delays dislocation movement and activates extra slip systems during plastic deformation.

(2) *Fracture behavior*. The disparity in intrinsic strength and modulus between reinforcement and matrix leads to crack nucleation primarily near the interface. Early failure of MMCs occurs when 1D reinforcements are agglomerated or the interfacial bonding with the matrix is weak. Therefore, the uniform dispersion of 1D reinforcements and the strong interface combination with the matrix collectively contribute to delaying the propagation and proliferation of cracks. During plastic deformation, the 1D reinforcements can bear loads, absorb energy from crack nucleation, and even fracture dissipate energy. As cracks propagate, reinforcements with a high aspect ratio can impede their progress by passivating the crack tips. Furthermore, the fracture behavior of MMCs reinforced with 1D reinforcements are different at high temperatures. Liu et al. [135] found that the pulled-out CNTs were spotted on the fractured surfaces at room and high temperature, but with different shapes and morphologies. Specifically, the pulled-out CNTs exhibit a curly shape at room temperature, while they are straight at high temperatures. Moreover, the pulled-out CNTs are covered by copper matrix, indicating a shift in fracture behavior from the failure of CNTs/Cu interface to Cu matrix at high temperature through the *in situ* tensile test. Consequently, this means that the fracture behavior of MMCs at high temperatures depends on the strength of the matrix rather than the 1D reinforcements/metal matrix interface.

The distribution of 1D reinforcements can also significantly affect fracture behavior. During plastic deformation, cracks preferentially nucleate near 1D reinforcements in the hard phase due to the local stress concentration. In the propagation process of crack, the 1D reinforcements with a large aspect ratio can hinder micro-cracks effectively [49]. Additionally, the non-uniform distribution of the 1D reinforcements may result in overlapping of the plastic deformation zone near reinforcements, resulting in crack tip passivation. As strain increases, the microcracks adjacent to 1D reinforcements gradually merge into the primary cracks, which propagate along the periphery of the hard phase. Upon reaching the interface between hard and soft phases, passivation of the primary crack occurs due to plastic deformation in the soft phase. The assurance of high plasticity and toughness in MMCs reinforced with non-uniform distribution 1D reinforcements is attributed to the multiple passivation and deflection mechanisms that occur during crack growth and propagation [20].

6.2.3. Two-dimensional reinforcements

(1) *Dislocation behavior*. Different from 0D and 1D reinforcements, the larger surface area of 2D reinforcements makes the mobile dislocations neither shear nor bypass them during the deformation process of the composites. In this case, 2D reinforcements with a larger specific surface area exhibit superior dislocation-hindering ability [93]. The simulation results of MD demonstrate that the motion of dislocation is frequently impeded by the central region of 2D reinforcements during their interaction. Conversely, it is often observed that the edge of 2D reinforcements serves as a nucleation site for dislocations [82].

The dislocation behavior can be influenced by the interfacial bonding strength, which is in turn affected by the surface roughness and shape of 2D reinforcements [79,136]. The principle they adhere to is to optimize the interaction with dislocations by enhancing the interfacial strength between 2D reinforcements and matrix. In addition, it is worth noting that chemical modification on the surface of GN is another effective technique to increase the roughness of the GN surface and consequently the interfacial interaction with the matrix.

What's more, MD simulations show that dislocation tends to propagate along the 2D reinforcements during quasi-static deformation, and the edge of 2D reinforcements can act as the dislocation source [82]. In contrast, in high-strain rate deformation, the dislocation can propagate across GN under the action of impact breakage [90]. In addition, the slip of dislocation can be transformed into stacking faults and deforming twins with the assistance of the GN/metal interface [95].

(2) *Fracture behavior*. The influence of 2D reinforcements on the fracture behavior of MMCs can be divided into two aspects: intrinsic effect and extrinsic effect. On the one hand, the 2D reinforcements with large specific surface areas restrict dislocation termination at the reinforcements/metal interface, leading to stress concentration at the interface. The presence of stress concentration at the interface, unlike 0D and 1D reinforcements, does not necessarily result in premature failure of MMCs when the interface is well bonded [91]. The geometry and variability of 2D reinforcements facilitate the initiation of partial dislocations at the interface. Moreover, the interface can also serve as a source for emitting partial dislocations, leading to the formation of LC locks. These LC locks, along with 2D reinforcements, further act as barriers to hinder dislocation movement, enhancing the

work-hardening capability of MMCs [90]. On the other hand, during the process of crack propagation, 2D reinforcements have the ability to effectively bridge and deflect the crack, further dissipating the energy of crack propagation [94].

6.2.4. Three-dimensional reinforcements

(1) *Dislocation behavior.* The 3D reinforcements are widely distributed in the 3D space of MMCs, which expands the dimension of reinforcements and leads to the complexity of interaction between 3D reinforcements, defects, and matrix due to generalized aspect ratio or specific surface area of 3D reinforcements and rich 3D reinforcements/matrix interfaces. Consequently, these will inevitably result in distinct deformation mechanisms within MMCs. Specifically, in the process of deformation of MMCs under load, 3D reinforcements have the ability to control grain boundary deformation or co-deform themselves with the matrix rather than solely relying on dislocation slip. For example, in the dual-phase Cu-B nanocomposite film, the deformation mechanisms for crystalline metals and amorphous solids are different. The former is dominated by dislocation and GB movement, while the latter is mainly decided by the formation of shear bands and microcrack propagation. During the deformation process, the 3D amorphous framework imposes constraints on propagation by the ledges and solute atoms at the grain-complexion interface and augments the flow stress required for dislocation motion (Fig. 18b). Secondly, the generation and accumulation of GNDs near 3D reinforcements/metal interfaces play a pivotal role in accommodating the strain gradient and sustaining a high strain-hardening rate during plastic deformation [115].

(2) *Fracture behavior.* Expending the energy required for crack nucleation or crack propagation is an effective strategy to improve the plasticity and toughness of MMCs. For 3D reinforcements, the macroscopic continuous spatial distribution leads to dislocations that are incapable of bypassing and consequently accumulate at the reinforcement/metal interface, resulting in a pronounced external toughening effect [22]. Meanwhile, 3D reinforcements can alleviate stress concentration within the matrix during deformation, either through their self-deformation or modulating grain boundary deformation, which serves to reduce dislocation nucleation as an intrinsic toughening mechanism. For example, it is reported that the Ti_2Cu/β shells can also stabilize the nanostructure under thermomechanical coupling conditions, which enabled the material to present superplasticity at elevated temperatures (Fig. 18c). Regions with larger strains always correspond to the place where significant phase interface slip occurs, therefore, the superplastic deformation should be governed by phase boundary sliding. Simultaneously, within the Cu-C system, the interlayer slippage of GN exhibits a propensity to mitigate stress concentration and reduce crack nucleation, which is anticipated to be further applied in 3D GN networks [137].

7. Conclusions and outlooks

7.1. Conclusions

This review outlines the four distinct dimensional reinforcements (0D, 1D, 2D and 3D) in MMCs and provides a concise overview of their synthesis processes and properties. It comprehensively summarizes and compares the strengthening mechanisms, toughening mechanisms, and deformation behavior related to the dimensional variance of reinforcements in MMCs, while also organizing and summarizing the influential factors. The primary advancements in research can be succinctly summarized as follows:

(1) For MMCs reinforced with 0D reinforcements, the pursuit of breaking the tradeoff between strength and plasticity has led researchers to focus on the dispersion of 0D reinforcements or integration of reducing particle size, achieving uniform distribution, and enhancing interface bonding strength with matrix, rather than using a single approach. The dispersion, size, interface, and distribution of 0D reinforcements all exert a profound influence on the ultimate properties of composites. In particular, the non-uniform distribution of 0D reinforcements such as isolate, laminate and QCNL can result in the overlap of plastic influence zones of particles, leading to variations in work hardening ability, dislocation action mechanisms, and crack behavior within MMCs.

(2) For MMCs reinforced with 1D reinforcements, the position, length, aspect ratio and orientation of 1D reinforcements have a significant influence on the strengthening effect of MMCs, resulting in different strengthening and toughening mechanisms and deformation behavior. Furthermore, the new non-uniform distribution of reinforcements and the use of hybrid reinforcement such as 1D+0D and 1D+2D have increasingly garnered attention as research focal points, yielding significant advancements in achieving a harmonious balance between the strength and functional properties of MMCs, including electrical and thermal conductivity.

(3) For MMCs reinforced with 2D reinforcements, in addition to GN, which remains a prominent area of research, BN, MXene, MAX phases, etc. have also been incorporated into MMCs as novel 2D reinforcements in order to achieve synergistically enhanced mechanical and functional properties. The shape, size, surface quality, specific surface area, and interface of the 2D reinforcements significantly influence the strengthening effect of MMCs. Namely, the extensive surface area of 2D reinforcements can generate a multitude of interfaces within the matrix, significantly impeding dislocation movement and alleviating stress concentration at the grain boundary. Simultaneously, the non-uniform distribution of 2D reinforcements along grain boundary can mitigate crack nucleation, while serving as an effect of deflection and bridge on the crack.

(4) For MMCs reinforced with 3D reinforcements formed by the continuous composition of precipitates or the assembly of precursor powders, 3D continuity in the space of MMCs is the basic definition and essential feature, and also the vital function to the unique properties and mechanisms. The continuity of 3D reinforcements makes it possible for the properties of MMCs to transfer from micro to macro and expands the function region of reinforcements in MMCs due to the regulation of grain boundary behavior by 3D reinforcements, which leads to the different strengthening mechanisms, toughening mechanisms and deformation behavior, even unique physical and chemical properties. More precisely, the isotropy of composites is ensured by a continuous conduction pathway consisting of controllable 3D reinforcements. Simultaneously, the plastic deformation of the metal matrix can be coordinated by phase transformation or interlayer slip through the 3D reinforcements.

7.2. Outlooks

Currently, the investigation of multi-dimensional reinforcements in MMCs based on the distribution of reinforcements is predominantly limited to theoretical research and laboratory-scale applications, with a certain disparity between its extensive societal production and industrial implementation. Nevertheless, there are still promising prospects for advancement:

(1) Interdisciplinarity facilitates the multi-structure and cross-scale distribution of reinforcements. Multiscale simulation, artificial intelligence machine learning, and materiomics have the potential

to unveil concealed opportunities for the distribution of reinforcements in MMCs with enhanced strength and toughness at accelerated development rates through sustainable pathways, thereby augmenting the efficiency of materials design.

(2) Advanced synthesis technology facilitates the realization of the complex distribution of reinforcements. The successful incorporation of complex 3D or even higher-dimensional biological structures into MMCs, while preserving their structural integrity, presents a major challenge for researchers. The emergence of novel technologies such as 3D printing offers the potential for synthesizing complex configurations.

(3) Multi-scale simulations and advanced characterization techniques facilitate structural analysis. The incorporation of fine distribution of reinforcements at the micro-scale enhances the overall properties of MMCs. However, the delicate design also brings about challenges related to the microstructure characterization and theoretical analysis. It necessitates the use of tools such as atomic-scale characterization, *in situ* observation of interaction mechanisms, and the development of multi-scale theoretical models to better understand mechanical behavior.

CRediT authorship contribution statement

Yuhang Xia: Writing – original draft, Investigation, Data curation. **Xiang Zhang:** Writing – review & editing, Validation, Supervision, Conceptualization. **Dongdong Zhao:** Methodology. **Xudong Rong:** Visualization, Formal analysis. **Chunnian He:** Resources. **Naiqin Zhao:** Supervision, Project administration, Funding acquisition.

Declaration of competing interest

The authors declare that they have no known competing financial interests or personal relationships that could have appeared to influence the work reported in this paper.

Acknowledgments

The authors would like to acknowledge the financial support of the National Natural Science Foundation of China (Grant Nos. 52130105 and 52371013).

References

[1] A. Nieto, A. Bisht, D. Lahiri, C. Zhang, A. Agarwal, Graphene reinforced metal and ceramic matrix composites: a review, Int. Mater. Rev. 62 (2017) 241–302, https://doi.org/10.1080/09506608.2016.1219481.

[2] H. Chen, K. Kosiba, C. Suryanarayana, T. Lu, Y. Liu, Y. Wang, K.G. Prashanth, Feedstock preparation, microstructures and mechanical properties for laser-based additive manufacturing of steel matrix composites, Int. Mater. Rev. 68 (2023) 1192–1244, https://doi.org/10.1080/09506608.2023.2258664.

[3] P. Lava Kumar, A. Lombardi, G. Byczynski, S.V.S. Narayana Murty, B.S. Murty, L. Bichler, Recent advances in aluminium matrix composites reinforced with graphene-based nanomaterial: a critical review, Prog. Mater. Sci. 128 (2022) 100948, https://doi.org/10.1016/j.pmatsci.2022.100948.

[4] J.H. Bak, Y.D. Kim, S.S. Hong, B.Y. Lee, S.R. Lee, J.H. Jang, M. Kim, K. Char, S. Hong, Y.D. Park, High-frequency micromechanical resonators from aluminium-carbon nanotube nanolaminates, Nat. Mater. 7 (2008) 459–463, https://doi.org/10.1038/nmat2181.

[5] D.G. Papageorgiou, I.A. Kinloch, R.J. Young, Mechanical properties of graphene and graphene-based nanocomposites, Prog. Mater. Sci. 90 (2017) 75–127, https://doi.org/10.1016/j.pmatsci.2017.07.004.

[6] X. Rong, D. Zhao, X. Chen, X. Zhang, D. Wan, C. Shi, C. He, N. Zhao, Towards the work hardening and strain delocalization achieved via in-situ intragranular reinforcement in Al-CuO composite, Acta Mater. 256 (2023) 119110, https://doi.org/10.1016/j.actamat.2023.119110.

[7] M. Yang, Y. Liu, T. Fan, D. Zhang, Metal-graphene interfaces in epitaxial and bulk systems: a review, Prog. Mater. Sci. 110 (2020) 100652, https://doi.org/10.1016/j.pmatsci.2020.100652.

[8] D.J. Lloyd, Particle reinforced aluminium and magnesium matrix composites, Int. Mater. Rev. 39 (1994) 1–23, https://doi.org/10.1179/imr.1994.39.1.1.

[9] J. Hwang, T. Yoon, S.H. Jin, J. Lee, T.S. Kim, S.H. Hong, S. Jeon, Enhanced mechanical properties of graphene/copper nanocomposites using a molecular-level mixing process, Adv. Mater. 25 (2013) 6724–6729, https://doi.org/10.1002/adma.201302495.

[10] L. Jiang, H. Yang, J.K. Yee, X. Mo, T. Topping, E.J. Lavernia, J.M. Schoenung, Toughening of aluminum matrix nanocomposites via spatial arrays of boron carbide spherical nanoparticles, Acta Mater. 103 (2016) 128–140, https://doi.org/10.1016/j.actamat.2015.09.057.

[11] X. Bai, H. Xie, X. Zhang, D. Zhao, X. Rong, S. Jin, E. Liu, N. Zhao, C. He, Heat-resistant super-dispersed oxide strengthened aluminium alloys, Nat. Mater. 23 (2024) 747–754, https://doi.org/10.1038/s41563-024-01884-2.

[12] L. Chen, J. Peng, J. Xu, H. Choi, X. Li, Achieving uniform distribution and dispersion of a high percentage of nanoparticles in metal matrix nanocomposites by solidification processing, Scr. Mater. 69 (2013) 634–637, https://doi.org/10.1016/j.scriptamat.2013.07.016.

[13] J.G. Ke, R. Liu, Z.M. Xie, L.C. Zhang, X.P. Wang, Q.F. Fang, C.S. Liu, X.B. Wu, Ultrahigh strength, thermal stability and high thermal conductivity in hierarchical nanostructured Cu-W alloy, Acta Mater. 264 (2024) 119547, https://doi.org/10.1016/j.actamat.2023.119547.

[14] L. Chen, J. Xu, H. Choi, M. Pozuelo, X. Ma, S. Bhowmick, J. Yang, S. Mathaudhu, X. Li, Processing and properties of magnesium containing a dense uniform dispersion of nanoparticles, Nature 528 (2015) 539–543, https://doi.org/10.1038/nature16445.

[15] C. He, N. Zhao, C. Shi, X. Du, J. Li, H. Li, Q. Cui, An approach to obtaining homogeneously dispersed carbon nanotubes in Al powders for preparing reinforced Al-matrix composites, Adv. Mater. 19 (2007) 1128–1132, https://doi.org/10.1002/adma.200601381.

[16] X. Zhang, N. Zhao, C. He, The superior mechanical and physical properties of nanocarbon reinforced bulk composites achieved by architecture design-A review, Prog. Mater. Sci. 113 (2020) 100672, https://doi.org/10.1016/j.pmatsci.2020.100672.

[17] L.J. Huang, L. Geng, H. Peng, Microstructurally inhomogeneous composites: is a homogeneous reinforcement distribution optimal? Prog. Mater. Sci. 71 (2015) 93–168, https://doi.org/10.1016/j.pmatsci.2015.01.002.

[18] W. Li, X. Qian, J. Li, Phase transitions in 2D materials, Nat. Rev. Mater. 6 (2021) 829–846, https://doi.org/10.1038/s41578-021-00304-0.

[19] Y. Wang, L. Li, D. Hofmann, J.E. Andrade, C. Daraio, Structured fabrics with tunable mechanical properties, Nature 596 (2021) 238–243, https://doi.org/10.1038/s41586-021-03698-7.

[20] L. Liu, S. Li, D. Pan, D. Hui, X. Zhang, B. Li, T. Liang, P. Shi, A. Bahador, J. Umeda, K. Kondoh, S. Li, L. Gao, Z. Wang, G. Li, S. Zhang, R. Wang, W. Chen, Loss-free tensile ductility of dual-structure titanium composites via an interdiffusion and self-organization strategy, Proc. Natl. Acad. Sci. USA 120 (2023) e2302234120, https://doi.org/10.1073/pnas.2302234120.

[21] Z. Li, X. Fu, Q. Guo, L. Zhao, G. Fan, Z. Li, D. Xiong, Y. Su, D. Zhang, Graphene quality dominated interface deformation behavior of graphene-metal composite: the defective is better, Int. J. Plast. 111 (2018) 253–265, https://doi.org/10.1016/j.ijplas.2018.07.020.

[22] X. Zhang, Y. Xu, M. Wang, E. Liu, N. Zhao, C. Shi, D. Lin, F. Zhu, C. He, A powder-metallurgy-based strategy toward three-dimensional graphene-like network for reinforcing copper matrix composites, Nat. Commun. 11 (2020) 2775, https://doi.org/10.1038/s41467-020-16490-4.

[23] T.P.D. Rajan, R.M. Pillai, B.C. Pai, Reinforcement coatings and interfaces in aluminium metal matrix composites, J. Mater. Sci. 23 (1998) 3491–3503, https://doi.org/10.1023/A:1004674822751.

[24] B.Q. Han, Theory of high-strain-rate superplastic flow in particulate-reinforced aluminium composites, Philos. Mag. A 77 (1998) 1127–1157, https://doi.org/10.1080/01418619808214244.

[25] G. Liu, G.J. Zhang, F. Jiang, X.D. Ding, Y.J. Sun, J. Sun, E. Ma, Nanostructured high-strength molybdenum alloys with unprecedented tensile ductility, Nat. Mater. 12 (2013) 344–350, https://doi.org/10.1038/nmat3544.

[26] K. Lu, The future of metals, Science 328 (2010) 319–320, https://doi.org/10.1126/science.1185866.

[27] A. Heidarzadeh, S. Mironov, R. Kaibyshev, G. çam, A. Simar, A. Gerlich, F. Khodabakhshi, A. Mostafaei, D.P. Field, J.D. Robson, A. Deschamps, P.J. Withers, Friction stir welding/processing of metals and alloys: a comprehensive review on microstructural evolution, Prog. Mater. Sci. 117 (2021) 100752, https://doi.org/10.1016/j.pmatsci.2020.100752.

[28] Z. Li, Y. Zhang, Z. Zhang, Y. Cui, Q. Guo, P. Liu, S. Jin, G. Sha, K. Ding, Z. Li, T. Fan, H.M. Urbassek, Q. Yu, T. Zhu, D. Zhang, Y.M. Wang, A nanodispersion-in-nanograins strategy for ultra-strong, ductile and stable metal nanocomposites, Nat. Commun. 13 (2022) 5581, https://doi.org/10.1038/s41467-022-33261-5.

[29] I. Kaldre, A. Bojarevičs, I. Grants, T. Beinerts, M. Kalvāns, M. Milgrāvis, G. Gerbeth, Nanoparticle dispersion in liquid metals by electromagnetically induced acoustic cavitation, Acta Mater. 118 (2016) 253–259, https://doi.org/10.1016/j.actamat.2016.07.045.

[30] Y. Ma, A. Addad, G. Ji, M. Zhang, W. Lefebvre, Z. Chen, V. Ji, Atomic-scale investigation of the interface precipitation in a TiB2 nanoparticles reinforced Al-Zn-Mg-Cu matrix composite, Acta Mater. 185 (2020) 287–299, https://doi.org/10.1016/j.actamat.2019.11.068.

[31] Y. Ma, H. Chen, M. Zhang, A. Addad, Y. Kong, M.B. Lezaack, W. Gan, Z. Chen, G. Ji, Break through the strength-ductility trade-off dilemma in aluminum matrix composites via precipitation-assisted interface tailoring, Acta Mater. 242 (2023) 118470, https://doi.org/10.1016/j.actamat.2022.118470.

[32] X. Zhang, T. Chen, S. Ma, H. Qin, J. Ma, Overcoming the strength-ductility trade-off of an aluminum matrix composite by novel core-shell structured reinforcing particulates, Compos. Part B-Eng. 206 (2021) 108541, https://doi.org/10.1016/j.compositesb.2020.108541.

[33] M. Sun, P. Shen, Q. Jiang, Microstructures and mechanical characterizations of high-performance nacre-inspired Al/Al_2O_3 composites, Compos. Part A-Appl. 121 (2019) 465–473, https://doi.org/10.1016/j.compositesa.2019.04.007.

[34] W. Huo, C. Lei, Y. Du, G. Chang, M. Zhu, B. Chen, Y. Zhang, Superior strength-ductility synergy of (TiC + Ti5Si3)/Ti composites with nacre-inspired architecture, Compos. Part B-Eng. 240 (2022) 109991, https://doi.org/10.1016/j.compositesb.2022.109991.

[35] F. Zhang, T. Liu, Nanodiamonds reinforced titanium matrix nanocomposites with network architecture, Compos. Part B-Eng. 165 (2019) 143–154, https://doi.org/10.1016/j.compositesb.2018.11.110.

[36] R.O. Ritchie, The conflicts between strength and toughness, Nat. Mater. 10 (2011) 817–822, https://doi.org/10.1038/nmat3115.

[37] X. Luo, K. Zhao, X. He, Y. Bai, V. De Andrade, M. Zaiser, L. An, J. Liu, Evading strength and ductility trade-off in an inverse nacre structured magnesium matrix nanocomposite, Acta Mater. 228 (2022) 117730, https://doi.org/10.1016/j.actamat.2022.117730.

[38] S.M. Ma a, P. Zhang a, G. Ji b, Z. Chen a, G.A. Sun c, S.Y. Zhong a, V. Ji d, H.W. Wang, Microstructure and mechanical properties of friction stir processed Al-Mg-Si alloys dispersion-strengthened by nanosized TiB2 particles, J. Alloys Compd. 616 (2014) 128–136, https://doi.org/10.1016/j.jallcom.2014.07.092.

[39] X. Rong, D. Zhao, C. He, C. Shi, E. Liu, N. Zhao, Revealing the strengthening and toughening mechanisms of Al-CuO composite fabricated via in-situ solid-state reaction, Acta Mater. 204 (2021) 116524, https://doi.org/10.1016/j.actamat.2020.116524.

[40] B. Kaveendran, G.S. Wang, L.J. Huang, L. Geng, Y. Luo, H.X. Peng, In situ (Al_3Zrp+Al_2O_3np)/2024Al metal matrix composite with controlled reinforcement architecture fabricated by reaction hot pressing, Mater. Sci. Eng., A 583 (2013) 89–95, https://doi.org/10.1016/j.msea.2013.07.002.

[41] X. Wang, S. Li, Y. Han, G. Huang, J. Mao, W. Lu, Visual assessment of special rod-like α-Ti precipitates within the in situ TiC crystals and the mechanical responses of titanium matrix composites, Compos. Part B-Eng. 230 (2022) 109511, https://doi.org/10.1016/j.compositesb.2021.109511.

[42] D. Wang, J. Huang, C. Tan, W. Ma, Y. Zou, Y. Yang, Mechanical and corrosion properties of additively manufactured SiC-reinforced stainless steel, Mater. Sci. Eng., A 841 (2022) 143018, https://doi.org/10.1016/j.msea.2022.143018.

[43] S.R. Bakshi, D. Lahiri, A. Agarwal, Carbon nanotube reinforced metal matrix composites-a review, Int. Mater. Rev. 55 (2010) 41–64, https://doi.org/10.1179/095066009X12572530170543.

[44] K.S. Munir, P. Kingshott, C. Wen, Carbon nanotube reinforced titanium metal matrix composites prepared by powder metallurgy-A review, Crit. Rev. Solid State Mater. 40 (2014) 38–55, https://doi.org/10.1080/10408436.2014.929521.

[45] Q. Li, A. Viereckl, C.A. Rottmair, R.F. Singer, Improved processing of carbon nanotube/magnesium alloy composites, Compos. Sci. Technol. 69 (2009) 1193–1199, https://doi.org/10.1016/j.compscitech.2009.02.020.

[46] Z.Y. Liu, B.L. Xiao, W.G. Wang, Z.Y. Ma, Modelling of carbon nanotube dispersion and strengthening mechanisms in Al matrix composites prepared by high energy ball milling-powder metallurgy method, Compos. Part A-Appl. 94 (2017) 189–198, https://doi.org/10.1016/j.compositesa.2016.11.029.

[47] J.G. Park, D.H. Keum, Y.H. Lee, Strengthening mechanisms in carbon nanotube-reinforced aluminum composites, Carbon 95 (2015) 690–698, https://doi.org/10.1016/j.carbon.2015.08.112.

[48] R. Xu, Z. Tan, G. Fan, G. Ji, Z. Li, Q. Guo, Z. Li, D. Zhang, Microstructure-based modeling on structure-mechanical property relationships in carbon nanotube/aluminum composites, Int. J. Plast. 120 (2019) 278–295, https://doi.org/10.1016/j.ijplas.2019.05.006.

[49] B. Chen, J. Shen, X. Ye, L. Jia, S. Li, J. Umeda, M. Takahashi, K. Kondoh, Length effect of carbon nanotubes on the strengthening mechanisms in metal matrix composites, Acta Mater. 140 (2017) 317–325, https://doi.org/10.1016/j.actamat.2017.08.048.

[50] K. Ma, X.N. Li, K. Liu, X.G. Chen, Z.Y. Liu, B.L. Xiao, Z.Y. Ma, Improving the high-cycle fatigue strength of heterogeneous carbon nanotube/Al-Cu-Mg composites through grain size design in ductile-zones, Compos. Part B-Eng. 222 (2021) 109094, https://doi.org/10.1016/j.compositesb.2021.109094.

[51] C. Zhang, Y. Zeng, D. Yao, J. Yin, K. Zuo, Y. Xia, H. Liang, The improved mechanical properties of Al matrix composites reinforced with oriented β-Si_3N_4 whisker, J. Mater. Sci. Technol. 35 (2019) 1345–1353, https://doi.org/10.1016/j.jmst.2019.02.003.

[52] P. Qiu, J. Le, Y. Han, Y. Chen, G. Huang, J. Mao, L. Lei, W. Lu, Superior superplasticity and multiple accommodation mechanisms in TiB reinforced near-α titanium matrix composites, Compos. Part B-Eng. 238 (2022) 109940, https://doi.org/10.1016/j.compositesb.2022.109940.

[53] L.J. Huang, L. Geng, B. Wang, H.Y. Xu, B. Kaveendran, Effects of extrusion and heat treatment on the microstructure and tensile properties of in situ TiBw/Ti6Al4V composite with a network architecture, Compos. Appl. Sci. Manuf. 43 (2012) 486–491, https://doi.org/10.1016/j.compositesa.2011.11.014.

[54] Y. Hu, W. Cong, X. Wang, Y. Li, F. Ning, H. Wang, Laser deposition-additive manufacturing of TiB-Ti composites with novel three-dimensional quasi-continuous network microstructure: effects on strengthening and toughening, Compos. Part B-Eng. 133 (2018) 91–100, https://doi.org/10.1016/j.compositesb.2017.09.019.

[55] X. Zhang, C. Shi, E. Liu, F. He, L. Ma, Q. Li, J. Li, N. Zhao, C. He, In-situ space-confined synthesis of well-dispersed three-dimensional graphene/carbon nanotube hybrid reinforced copper nanocomposites with balanced strength and ductility, Compos. Appl. Sci. Manuf. 103 (2017) 178–187, https://doi.org/10.1016/j.compositesa.2017.09.010.

[56] S. Cui, C. Cui, S. Yang, S. Liu, Microstructure evolution and the mechanical properties of in-situ Ti_2AlCw-NbC@TiBx/TiAlNb composite with high performance, Compos. Part B-Eng. 234 (2022) 109689, https://doi.org/10.1016/j.compositesb.2022.109689.

[57] J. Le, Y. Han, M. Fang, S. Li, G. Huang, J. Mao, C.J. Boehlert, W. Lu, Microstructure evolution and the mechanical properties of in-situ Ti2AlCw-NbC@TiBx/TiAlNb composite with high performance, Compos. Part B-Eng. 247 (2022) 110317, https://doi.org/10.1016/j.compositesb.2022.109689.

[58] K. Ma, X.N. Li a, K. Liu b, X.G. Chen b, Z.Y. Liu a, B.L. Xiao a, Z.Y. Ma, Improving the high-cycle fatigue strength of heterogeneous carbon nanotube/Al-Cu-Mg composites through grain size design in ductile-zones, Compos. Part B-Eng. 222 (2021) 109094, https://doi.org/10.1016/j.compositesb.2021.109094.

[59] M.Y. Zhou, L.B. Ren, L.L. Fan, Y.W.X. Zhang, T.H. Lu, G.F. Quan, M. Gupta, Progress in research on hybrid metal matrix composites, J. Alloys Compd. 838 (2020) 155274, https://doi.org/10.1016/j.jallcom.2020.155274.

[60] Y. Shan, B. Pu, E. Liu, C. Shi, C. He, N. Zhao, In-situ synthesis of CNTs@Al_2O_3 wrapped structure in aluminum matrix composites with balanced strength and toughness, Mater. Sci. Eng., A 797 (2020) 140058, https://doi.org/10.1016/j.msea.2020.140058.

[61] X. Fu, Z. Tan, Z. Ma, Z. Li, G. Fan, D. Xiong, Z. Li, Powder assembly & alloying to CNT/Al-Cu-Mg composites with trimodal grain structure and strength-ductility synergy, Compos. Part B-Eng. 225 (2021) 109271, https://doi.org/10.1016/j.compositesb.2021.109271.

[62] L. Cao, B. Chen, J. Wan, K. Kondoh, B. Guo, J. Shen, J.S. Li, Superior high-temperature tensile properties of aluminum matrix composites reinforced with carbon nanotubes, Carbon 191 (2022) 403–414, https://doi.org/10.1016/j.carbon.2022.02.009.

[63] B. Guo, M. Song, X. Zhang, Y. Liu, X. Cen, B. Chen, W. Li, Exploiting the synergic strengthening effects of stacking faults in carbon nanotubes reinforced aluminum matrix composites for enhanced mechanical properties, Compos. Part B-Eng. 211 (2021) 108646, https://doi.org/10.1016/j.compositesb.2021.108646.

[64] Y. Meng, J. Feng, S. Han, Z. Xu, W. Mao, T. Zhang, J.S. Kim, I. Roh, Y. Zhao, D. Kim, Y. Yang, J. Lee, L. Yang, C. Qiu, S. Bae, Photonic van der Waals integration from 2D materials to 3D nanomembranes, Nat. Rev. Mater. 8 (2023) 498–517, https://doi.org/10.1038/s41578-023-00558-w.

[65] Y. Qi, M.A. Sadi, D. Hu, M. Zheng, Z. Wu, Y. Jiang, Y.P. Chen, Recent Progress in Strain Engineering on Van der Waals 2D Materials: Tunable Electrical, Electrochemical, Magnetic, and Optical Properties, Adv. Mater. 35 (2023), https://doi.org/10.1002/adma.202205714.

[66] A. Elbanna, H. Jiang, Q. Fu, J. Zhu, Y. Liu, M. Zhao, D. Liu, S. Lai, X.W. Chua, J. Pan, Z.X. Shen, L. Wu, Z. Liu, C. Qiu, J. Teng, 2DMaterial infrared photonics and plasmonics, ACS Nano 17 (2023) 4134–4179, https://doi.org/10.1021/acsnano.2c10705.

[67] S.C. Yoo, D. Lee, S.W. Ryu, B. Kang, H.J. Ryu, S.H. Hong, Recent progress in low-dimensional nanomaterials filled multifunctional metal matrix nanocomposites, Prog. Mater. Sci. 132 (2023) 101034, https://doi.org/10.1016/j.pmatsci.2022.101034.

[68] A.K. Geim, K.S. Novoselov, The rise of graphene, Nat. Mater. 6 (2007) 183–191, https://doi.org/10.1038/nmat1849.

[69] X. Zhang, C. Shi, E. Liu, F. He, L. Ma, Q. Li, J. Li, W. Bacsa, N. Zhao, C. He, Achieving high strength and high ductility in metal matrix composites reinforced with a discontinuous three-dimensional graphene-like network, Nanoscale 9 (2017) 11929–11938, https://doi.org/10.1039/C6NR07335B.

[70] K.S. Novoselov, V.I. Fal Ko, L. Colombo, P.R. Gellert, M.G. Schwab, K. Kim, A roadmap for graphene, Nature 490 (2012) 192–200, https://doi.org/10.1038/nature11458.

[71] J. Li, X. Zhang, M. Qian, Z. Jia, M. Imran, L. Geng, Inhibiting GNPs breakage during ball milling for a balanced strength-ductility match in GNPs/Al composites, Compos. Appl. Sci. Manuf. 166 (2023) 107410, https://doi.org/10.1016/j.compositesa.2022.107410.

[72] B. Pu, X. Zhang, X. Chen, X. Lin, D. Zhao, C. Shi, E. Liu, J. Sha, C. He, N. Zhao, Exceptional mechanical properties of aluminum matrix composites with heterogeneous structure induced by in-situ graphene nanosheet-Cu hybrids, Compos. Part B-Eng. 234 (2022) 109731, https://doi.org/10.1016/j.compositesb.2022.109731.

[73] W. Wang, F. Li, Y. Xu, K. Zhan, T. Wang, Z. Yang, Z. Wang, B. Zhao, Laminated Cu-GO-Cu composite foils with improved mechanical and thermal properties by alternating DC electro-deposition and electrophoresis, J. Mater. Res. Technol. 19 (2022) 1724–1739, https://doi.org/10.1016/j.jmrt.2022.05.166.

[74] J. Hwang, T. Yoon, S.H. Jin, J. Lee, T. Kim, S.H. Hong, S. Jeon, Enhanced mechanical properties of graphene/copper nanocomposites using a molecular-level mixing process, Adv. Mater. 25 (2013) 6724–6729, https://doi.org/10.1002/adma.201302495.

[75] S. Zhao, Y. Zhang, D. Chen, J. Yang, S. Kitipornchai, Enhanced thermal buckling resistance of folded graphene reinforced nanocomposites with negative thermal expansion: from atomistic study to continuum mechanics modelling, Compos. Struct. 279 (2022) 114872, https://doi.org/10.1016/j.compstruct.2021.114872.

[76] J. Li, X. Zhang, M. Qian, Z. Jia, M. Imran, L. Geng, Inhibiting GNPs breakage during ball milling for a balanced strength-ductility match in GNPs/Al composites, Compos. Appl. Sci. Manuf. 166 (2023) 107410, https://doi.org/10.1016/j.compositesa.2022.107410.

[77] A. Morvan, J. Grosseau-Poussard, N. Caillault, F. Delange, S. Roure, P. Lepretre, J. Silvain, Powder processing methodology for fabrication of Copper/Graphite composite materials with enhanced thermal properties, Compos. Appl. Sci. Manuf. 124 (2019) 105474, https://doi.org/10.1016/j.compositesa.2019.105474.

[78] X. Zhang, C. Shi, E. Liu, N. Zhao, C. He, Effect of interface structure on the mechanical properties of graphene nanosheets reinforced copper matrix composites, ACS Appl. Mater. Interfaces 10 (2018) 37586–37601, https://doi.org/10.1021/acsami.8b09799.
[79] S. Guo, X. Zhang, C. Shi, D. Zhao, C. He, N. Zhao, Continuous confined interfacial design in graphene/Cu composites with structural integrity enables improvement of comprehensive properties, Compos. Appl. Sci. Manuf. 169 (2023) 107525, https://doi.org/10.1016/j.compositesa.2023.107525.
[80] S. Guo, X. Zhang, C. Shi, D. Zhao, E. Liu, C. He, N. Zhao, Comprehensive performance regulation of Cu matrix composites with graphene nanoplatelets in situ encapsulated Al_2O_3 nanoparticles as reinforcement, Carbon 188 (2022) 81–94, https://doi.org/10.1016/j.carbon.2021.11.054.
[81] Z. Li, Q. Guo, Z. Li, G. Fan, D. Xiong, Y. Su, J. Zhang, D. Zhang, Enhanced mechanical properties of graphene (reduced graphene oxide)/aluminum composites with a bioinspired nanolaminated structure, Nano Lett. 15 (2015) 8077–8083, https://doi.org/10.1021/acs.nanolett.5b03492.
[82] F. Shuang, K.E. Aifantis, Dislocation-graphene interactions in Cu/graphene composites and the effect of boundary conditions: a molecular dynamics study, Carbon 172 (2021) 50–70, https://doi.org/10.1016/j.carbon.2020.09.043.
[83] V.H. Vardanyan, H.M. Urbassek, Morphology of graphene flakes in Ni-graphene nanocomposites and its influence on hardness: an atomistic study, Carbon 185 (2021) 660–668, https://doi.org/10.1016/j.carbon.2021.09.065.
[84] L. Zhao, Q. Guo, Z. Li, D. Xiong, S. Osovski, Y. Su, D. Zhang, Strengthening and deformation mechanisms in nanolaminated graphene-Al composite micro-pillars affected by graphene in-plane sizes, Int. J. Plast. 116 (2019) 265–279, https://doi.org/10.1016/j.ijplas.2019.01.006.
[85] C. Androulidakis, E.N. Koukaras, J. Rahova, K. Sampathkumar, J. Parthenios, K. Papagelis, O. Frank, C. Galiotis, Wrinkled few-layer graphene as highly efficient load bearer, ACS Appl. Mater. Interfaces 9 (2017) 26593–26601, https://doi.org/10.1021/acsami.7b07547.
[86] S. Zhao, Y. Zhang, J. Yang, S. Kitipornchai, Significantly improved interfacial shear strength in graphene/copper nanocomposite via wrinkles and functionalization: a molecular dynamics study, Carbon 174 (2021) 335–344, https://doi.org/10.1016/j.carbon.2020.12.026.
[87] Y. Jiang, Z. Tan, G. Fan, L. Wang, D. Xiong, Q. Guo, Y. Su, Z. Li, D. Zhang, Reaction-free interface promoting strength-ductility balance in graphene nanosheet/Al composites, Carbon 158 (2020) 449–455, https://doi.org/10.1016/j.carbon.2019.11.010.
[88] K. Chu, F. Wang, Y. Li, X. Wang, D. Huang, H. Zhang, Interface structure and strengthening behavior of graphene/CuCr composites, Carbon 133 (2018) 127–139, https://doi.org/10.1016/j.carbon.2018.03.018.
[89] X.J. Long, B. Li, L. Wang, J.Y. Huang, J. Zhu, S.N. Luo, Shock response of Cu/graphene nanolayered composites, Carbon 103 (2016) 457–463, https://doi.org/10.1016/j.carbon.2016.03.039.
[90] D. Lin, M. Motlag, M. Saei, S. Jin, R.M. Rahimi, D. Bahr, G.J. Cheng, Shock engineering the additive manufactured graphene-metal nanocomposite with high density nanotwins and dislocations for ultra-stable mechanical properties, Acta Mater. 150 (2018) 360–372, https://doi.org/10.1016/j.actamat.2018.03.013.
[91] X. Zhang, D. Zhao, R. Shi, S. Zhu, L. Ma, C. He, N. Zhao, Investigations on the interface-dominated deformation mechanisms of two-dimensional MAX-phase $Ti_3Al(Cu)C_2$ nanoflakes reinforced copper matrix composites, Acta Mater. 240 (2022) 118363, https://doi.org/10.1016/j.actamat.2022.118363.
[92] M.A. Meyers, P. Chen, A.Y. Lin, Y. Seki, Biological materials: structure and mechanical properties, Prog. Mater. Sci. 53 (2008) 1–206, https://doi.org/10.1016/j.pmatsci.2007.05.002.
[93] D. Xiong, M. Cao, Q. Guo, Z. Tan, G. Fan, Z. Li, D. Zhang, Graphene-and-Copper artificial nacre fabricated by a preform impregnation process: bioinspired strategy for strengthening-toughening of metal matrix composite, ACS Nano 9 (2015) 6934–6943, https://doi.org/10.1021/acsnano.5b01067.
[94] Y. Zhang, F.M. Heim, J.L. Bartlett, N. Song, D. Isheim, X. Li, Bioinspired, graphene-enabled Ni composites with high strength and toughness, Sci. Adv. 5 (2019) v5577, https://doi.org/10.1126/sciadv.aav5577.
[95] Y. Peng, G. Luo, Y. Hu, D. Xiong, Dynamic deformation mechanism in submicro-laminated copper with interlamellar graphene multilayers, Acta Mater. 252 (2023) 118941, https://doi.org/10.1016/j.actamat.2023.118941.
[96] H. Wang, W. Song, M. Liu, S. Zhang, L. Ren, D. Qiu, X. Chen, K. Yang, Nat. Commun. 13 (2022) 2034, https://doi.org/10.1038/s41467-022-29782-8.
[97] L. Lu, X. Chen, X. Huang, K. Lu, Revealing the maximum strength in nanotwinned copper, Science 323 (2009) 607–610. https://www.science.org/doi/10.1126/science.1167641.
[98] X.C. Liu, H.W. Zhang, K. Lu, Strain-induced ultrahard and ultrastable nanolaminated structure in nickel, Science 342 (2013) 337–340. https://www.science.org/doi/10.1126/science.1242578.
[99] V.Y. Gertsman, R. Birringer, On the room-temperature grain growth in nanocrystalline copper, Scripta Metall. Mater. 30 (1994) 577–581, https://doi.org/10.1016/0956-716X(94)90432-4.
[100] J.R. Weertman, Retaining the nano in nanocrystalline alloys, Science 337 (2012) 921–922. https://www.science.org/doi/10.1126/science.1226724.
[101] K.A. Darling, M. Rajagopalan, M. Komarasamy, M.A. Bhatia, B.C. Hornbuckle, R.S. Mishra, K.N. Solanki, Extreme creep resistance in a microstructurally stable nanocrystalline alloy, Nature 537 (2016) 378–381, https://doi.org/10.1038/nature19313.
[102] M. Zhang, Q. Yu, Z. Liu, J. Zhang, G. Tan, D. Jiao, W. Zhu, S. Li, Z. Zhang, R. Yang, R.O. Ritchie, 3D printed Mg-NiTi interpenetrating-phase composites with high strength, damping capacity, and energy absorption efficiency, Sci. Adv. 6 (2020) a5581. https://www.science.org/doi/10.1126/sciadv.aba5581.
[103] X. Miao, C. Wang, T. Liao, S. Ju, J. Zha, W. Wang, J. Liu, Y. Zhang, Q. Ren, F. Xu, L. Caron, Novel magnetocaloric composites with outstanding thermal conductivity and mechanical properties boosted by continuous Cu network, Acta Mater. 242 (2023) 118453, https://doi.org/10.1016/j.actamat.2022.118453.
[104] T. Li, Y. Wang, M. Yang, H. Hou, S. Wu, High strength and conductivity copper/graphene composites prepared by severe plastic deformation of graphene coated copper powder, Mater. Sci. Eng., A 826 (2021) 141983, https://doi.org/10.1016/j.msea.2021.141983.
[105] K. Lu, L. Lu, S. Suresh, Strengthening materials by engineering coherent internal boundaries at the nanoscale, Science 324 (2009) 349–352, https://doi.org/10.1126/science.11596.
[106] M.A. Meyers, A. Mishra, D.J. Benson, Mechanical properties of nanocrystalline materials, Prog. Mater. Sci. 51 (2006) 427–556, https://doi.org/10.1016/j.pmatsci.2005.08.003.
[107] K. Ming, Z. Zhu, W. Zhu, B. Fang, B. Wei, P.K. Liaw, X. Wei, J. Wang, S. Zheng, Enhancing strength and ductility via crystalline-amorphous nanoarchitectures in TiZr-based alloys, Sci. Adv. 8 (2022) m2884, https://doi.org/10.1126/sciadv.abm2884.
[108] H. Lv, X. Gao, K. Zhang, M. Wen, X. He, Z. Wu, C. Liu, C. Chen, W. Zheng, Bamboo-like dual-phase nanostructured copper composite strengthened by amorphous boron framework, Nat. Commun. 14 (2023) 4638, https://doi.org/10.1038/s41467-023-40580-8.
[109] F. Zhang, J. Wang, T. Liu, C. Shang, Enhanced mechanical properties of few-layer graphene reinforced titanium alloy matrix nanocomposites with a network architecture, Mater. Des. 186 (2020) 108330, https://doi.org/10.1016/j.matdes.2019.108330.
[110] B. Li, D. Lin, X. Zhang, D. Zhao, C. He, N. Zhao, Exceptional dynamic compressive properties of bio-inspired three-dimensional interlocking graphene network reinforced copper matrix composites, Compos. Appl. Sci. Manuf. 176 (2024) 107856, https://doi.org/10.1016/j.compositesa.2023.107856.
[111] N. Nan, J. Li, X. Zhang, D. Zhao, F. Zhu, C. He, N. Zhao, Achieving excellent thermal stability in continuous three-dimensional graphene network reinforced copper matrix composites, Carbon 212 (2023) 118153, https://doi.org/10.1016/j.carbon.2023.118153.
[112] Y. Yang, M. Liu, J. Du, W. Zhang, S. Zhou, W. Ren, Q. Zhou, L. Shi, Construction of graphene network in Ni matrix composites: a molecular dynamics study of densification process, Carbon 191 (2022) 55–66, https://doi.org/10.1016/j.carbon.2022.01.044.
[113] Y. Yang, M. Liu, S. Zhou, W. Ren, Q. Zhou, W. Zhang, Strengthening behaviour of continuous graphene network in metal matrix composites, Carbon 182 (2021) 825–836, https://doi.org/10.1016/j.carbon.2021.06.067.
[114] Z. Gao, T. Zuo, M. Wang, L. Zhang, B. Da, Y. Ru, J. Xue, Y. Wu, L. Han, L. Xiao, In-situ graphene enhanced copper wire: a novel electrical material with simultaneously high electrical conductivity and high strength, Carbon 186 (2022) 303–312, https://doi.org/10.1016/j.carbon.2021.10.015.
[115] G. Li, J. Jiang, H. Ma, R. Zheng, S. Gao, S. Zhao, C. Ma, K. Ameyama, B. Ding, X. Li, Superior strength–ductility synergy in three-dimensional heterogeneous-nanostructured metals, Acta Mater. 256 (2023) 119143, https://doi.org/10.1016/j.actamat.2023.119143.
[116] Y. Mu, L. He, S. Deng, Y. Jia, Y. Jia, G. Wang, Q. Zhai, P.K. Liaw, C. Liu, A high-entropy alloy with dislocation-precipitate skeleton for ultrastrength and ductility, Acta Mater. 232 (2022) 117975, https://doi.org/10.1016/j.actamat.2022.117975.
[117] X. Liu, Z. Liu, Y. Liu, Z. Zafar, Y. Lu, X. Wu, Y. Jiang, Z. Xu, Z. Guo, S. Li, Achieving high strength and toughness by engineering 3D artificial nacre-like structures in Ti6Al4V-Ti metallic composite, Compos. Part B-Eng. 230 (2022) 109552, https://doi.org/10.1016/j.compositesb.2021.109552.
[118] Y. Zhao, Z. Ma, L. Yu, Y. Liu, New alloy design approach to inhibiting hot cracking in laser additive manufactured nickel-based superalloys, Acta Mater. 247 (2023) 118736, https://doi.org/10.1016/j.actamat.2023.118736.
[119] J. Hu, Y.N. Shi, X. Sauvage, G. Sha, K. Lu, Grain boundary stability governs hardening and softening in extremely fine nanograined metals, Science 355 (2017) 1292–1296. https://www.science.org/doi/10.1126/science.aal5166.
[120] K. Wang, S. Cheng, Q. Hu, F. Yu, Y. Cheng, K. Huang, H. Yuan, J. Jiang, W. Li, J. Li, S. Xu, J. Yin, Y. Qi, Z. Liu, Vertical graphene-coated Cu wire for enhanced tolerance to high current density in power transmission, Nano Res. 15 (2022) 9727–9733, https://doi.org/10.1007/s12274-021-3953-3.
[121] S. Scudino, G. Liu, M. Sakaliyska, K.B. Surreddi, J. Eckert, Powder metallurgy of Al-based metal matrix composites reinforced with β-Al_3Mg_2 intermetallic particles: analysis and modeling of mechanical properties, Acta Mater. 57 (2009) 4529–4538, https://doi.org/10.1016/j.actamat.2009.06.017.
[122] C. Han, R. Babicheva, J.D.Q. Chua, U. Ramamurty, S.B. Tor, C. Sun, K. Zhou, Microstructure and mechanical properties of (TiB+TiC)/Ti composites fabricated in situ via selective laser melting of Ti and B4C powders, Addit. Manuf. 36 (2020) 101466, https://doi.org/10.1016/j.addma.2020.101466.
[123] K. Ma, H. Wen, T. Hu, T.D. Topping, D. Isheim, D.N. Seidman, E.J. Lavernia, J.M. Schoenung, Mechanical behavior and strengthening mechanisms in ultrafine grain precipitation-strengthened aluminum alloy, Acta Mater. 62 (2014) 141–155, https://doi.org/10.1016/j.actamat.2013.09.042.
[124] M. Muñoz-Morris, C. Garcia Oca, D. Morris, An analysis of strengthening mechanisms in a mechanically alloyed, oxide dispersion strengthened iron aluminide intermetallic, Acta Mater. 50 (2002) 2825–2836, https://doi.org/10.1016/S1359-6454(02)00101-5.
[125] Z. Zhang, T. Topping, Y. Li, R. Vogt, Y. Zhou, C. Haines, J. Paras, D. Kapoor, J.M. Schoenung, E.J. Lavernia, Mechanical behavior of ultrafine-grained Al

composites reinforced with B_4C nanoparticles, Scr. Mater. 65 (2011) 652–655, https://doi.org/10.1016/j.scriptamat.2011.06.037.
[126] Y. Estrin, Y. Beygelzimer, R. Kulagin, P. Gumbsch, P. Fratzl, Y. Zhu, H. Hahn, Architecturing materials at mesoscale: some current trends, Mater. Res. Lett. 9 (2021) 399–421, https://doi.org/10.1080/21663831.2021.1961908.
[127] C. Goh, J. Wei, L. Lee, M. Gupta, Properties and deformation behaviour of Mg-Y_2O_3 nanocomposites, Acta Mater. 55 (2007) 5115–5121, https://doi.org/10.1016/j.actamat.2007.05.032.
[128] H.L. Cox, The elasticity and strength of paper and other fibrous materials, British, J. Appl. Phys. 3 (1952) 72. https://iopscience.iop.org/article/10.1088/0508-3443/3/3/302.
[129] H.J. Ryu, S.I. Cha, S.H. Hong, Generalized shear-lag model for load transfer in SiC/Al metal-matrix composites, J. Mater. Res. 18 (2003) 2851–2858, https://doi.org/10.1557/JMR.2003.0398.
[130] X. Li, L. Lu, J. Li, X. Zhang, H. Gao, Mechanical properties and deformation mechanisms of gradient nanostructured metals and alloys, Nat. Rev. Mater. 5 (2020) 706–723, https://doi.org/10.1038/s41578-020-0212-2.
[131] H. Wang, R. Kou, H. Yi, S. Figueroa, K.S. Vecchio, Mesoscale hetero-deformation induced (HDI) stress in FeAl-based metallic-intermetallic laminate (MIL) composites, Acta Mater. 213 (2021) 116949, https://doi.org/10.1016/j.actamat.2021.116949.
[132] C. Jiao, Z. Yao, Y. Han, Extrusion deformation texture of SiC-W/Al composites, J. Mater. Sci. Technol. 8 (1992) 25–29. https://www.jmst.org/EN/Y1992/V8/I1/25.
[133] B. Sadeghi, Z. Tan, J. Qi, Z. Li, X. Min, Z. Yue, G. Fan, Enhanced mechanical properties of CNT/Al composite through tailoring grain interior/grain boundary affected zones, Compos. Part B-Eng. 223 (2021) 109133, https://doi.org/10.1016/j.compositesb.2021.109133.
[134] Y. Wu, C. Zhou, R. Wu, L. Sun, C. Lu, Y. Xiao, Z. Su, M. Gong, K. Ming, K. Liu, C. Gu, W. Yang, J. Wang, G. Wu, Synergistic strengthening of Al–SiC composites by nano-spaced SiC-nanowires and the induced high-density stacking faults, Compos. Part B-Eng. 250 (2023) 110458, https://doi.org/10.1016/j.compositesb.2022.110458.
[135] J. Liu, G. Fan, Z. Tan, Q. Guo, Y. Su, Z. Li, D. Xiong, Mechanical properties and failure mechanisms at high temperature in carbon nanotube reinforced copper matrix nanolaminated composite, Compos. Appl. Sci. Manuf. 116 (2019) 54–61, https://doi.org/10.1016/j.compositesa.2018.10.022.
[136] S. Guo, X. Zhang, C. Shi, D. Zhao, C. He, N. Zhao, Fully exploiting the role of heterogeneous grain structure in graphene nanoplatelets reinforced Cu matrix composites through interfacial structure design, Compos. Commun. 35 (2022) 101287, https://doi.org/10.1016/j.coco.2022.101287.
[137] X. Zhang, D. Xiong, Y. Liu, Y. Jia, Y. Zhang, M. Zhou, H. Liu, Y. Geng, X. Wang, P. Liu, X. Song, D. Zhang, Multilayer graphene interface enabled ultrahigh extensibility for high performance bulk nanostructured copper, Acta Mater. 267 (2024) 119710, https://doi.org/10.1016/j.actamat.2024.119710.